BRITISH GEOLOGICAL SURVEY
Natural Environment Research Council

Technical Report WN/95/11

Hydrogeological classification of superficial clays: Apparent resistivity measurements from the Garboldisham, Norfolk pilot study area.

by

J P Busby, R J Peart, P I Meldrum and D Beamish

Bibliographic Reference

Busby J P, Peart R J, Meldrum P I, and Beamish D, 1995
Hydrogeological classification of superficial clays:
Apparent resistivity measurements from the
Garboldisham, Norfolk pilot study area.

British Geological Survey
Technical Report WN/95/11

Technical Report WN/95/11

Hydrogeological classification of superficial clays: Apparent resistivity measurements from the Garboldisham, Norfolk pilot study area.

Engineering Geology & Geophysics Group
British Geological Survey
Keyworth
Nottingham
NG12 5GG

tel. (0115) 9363100 Fax (0115) 9363145

Summary

Three types of apparent resistivity measurements have been undertaken at the Garboldisham pilot study area in Norfolk in support of the superficial clays programme. Resistivity soundings have established the intrinsic resistivities for the strata encountered. Cover sand (possibly mixed with glacial sand) of resistivities 100 - 200 ohm.m overlies till of resistivities 22 - 32 ohm.m which lies directly on chalk of resistivities 65 - 85 ohm.m. At the sounding sites, depth to chalk is in the range 11 - 15 m.

Azimuthal apparent resistivity measurements were made in an attempt to identify fracture sets within the till and to establish the degree of fracturing between measurement sites. These fracture sets will have an important influence on the hydrogeological regime. At only two of the five sites investigated was a fracture trend recognised and this had an orientation of 210° - 225°. There was an indication of a change in the intensity of fracturing between the two sites. The results indicate that there is either a lack of fracturing with a consistent trend within the till or that there is an insufficient resistivity contrast between the conductive till and the fractures.

Detailed dipole-dipole apparent resistivity measurements undertaken with the BGS RESCAN system were able to map the thickness of cover sand over a suspected sand channel. The sand body has a north - south orientation with a variable depth to the till surface. Maximum depths are up to two metres. The effectiveness of the resistivity technique for mapping sand lying on till has been demonstrated in this study.

Contents

List of Figures

1. Introduction

This report is an account of some apparent resistivity measurements taken at the Garboldisham pilot study area in Norfolk in support of the Hydrogeological Classification of Superficial Clays programme; a co-funded programme of research between the BGS and the National Rivers Authority. The geology of the area has been studied in detail (Hopson and Morigi, 1993) and this information was used for the siting of the geophysics.

There are two areas where it was hoped that apparent resistivity measurements would contribute to an understanding of the study area. The Lowestoft Till, which covers the site, is known to be fractured and these fractures may follow a uniform orientation. As a result some of the physical properties of the till may be anisotropic and this can be exploited by an azimuthal measurement to map the orientation of the fractures or the preferred connectivity path through the fracture system should there be more than one fracture set. The degree of anisotropy between measurement sites may also be an indication of the intensity of fracturing.

Secondly the till is covered by a variable thickness of cover sand, which is usually less than one metre thick, but in channels or hollows may attain several metres thickness. In places there is also a glacial sand which may have become mixed with the cover sand. The sand has important implications for the hydrogeology. The till is known to be conductive (Hopson and Morigi, 1993) hence there should be a large conductivity contrast between the till and the sand. An area was selected over which detailed apparent resistivity measurements were taken in an attempt to map the interface between the till and the sand.

Field work was undertaken over a six day period between 8th - 13th February 1995.

2. Background and objectives of the study

The detailed mapping of Hopson and Morigi (1993) has defined the areas of till and glacial sand. Where a significant covering of sand occurs (glacial or cover sand) a perched water table may result with a consequent saturation of the underlying till. This till is usually oxidised and fractured whereas the deeper till is less oxidised and less fractured. Since the till lies directly on the chalk, vertical movement of the water table in the chalk will also result in an oxidised and fractured till layer at the base of the till. The purpose of the azimuthal resistivity measurements was to attempt to measure the fracture direction in the oxidised till (assuming that the fractures develop as a set with a preferred orientation) and to compare the fracture intensity from one site to another.

Hopson and Morigi (1993) conducted some ground conductivity measurements with the Geonics EM31. These data indicated a linear, north trending resistive feature which may be due to the presence of a sand body or channel. The detailed apparent resistivity measurements were taken with the BGS RESCAN system on profiles perpendicular to the resistive feature (see Figure 1). These data have been interpreted in order to provide estimates of the thickness of sand.

3. Methodology

With the resistivity technique a direct current is made to flow in the ground between two current electrodes A and B. A potential difference is measured between another two electrodes M and N, located in-line with AB. From the measured current and voltage a resistance is calculated which, when multiplied by a factor depending on the location of the electrodes, produces an apparent resistivity measured in Ohm.m.

Three types of apparent resistivity measurements were taken at Garboldisham; azimuthal measurements for fracture mapping; detailed measurements along profiles employing the dipole-dipole array for mapping the sand layer and resistivity soundings for estimating the thickness of the till and to provide intrinsic resistivities of the till and sand.

3.1 Azimuthal apparent resistivity

Azimuthal apparent resistivity measurements are obtained by expanding a co-linear four electrode array about a central point along a fixed azimuth. The procedure is then repeated along other azimuths until the electrode array has been effectively rotated through 180°. The apparent resistivities for any one electrode spacing are then plotted against azimuth in a polar diagram. If this is circular then either there are no measurable fracture sets or the volume of strata investigated was insufficient (because the electrode array spacing was too small) for the strata to behave anisotropically. If a distinct ellipse results then the major axis of the ellipse is coincident with the strike of the fractures. If a multiple peaked pattern is observed then the azimuth of the peaks indicates the strike of more than one fracture set. The amplitude range of the polar diagrams is linear from the minimum recorded value (inner diameter) to the maximum recorded value (outer diameter), in order to emphasise the anisotropy.

The degree of anisotropy is expressed quantitatively as a percentage variation about the average value recorded, ie.

$$\pm\ 0.5\ [(a_{max} - a_{min})/(\Sigma a/n)]\ 100\%$$

where "a" is apparent resistivity and "n" is the number of measurements plotted in the polar diagram.

The theoretical development of the response of a homogeneous but anisotropic rock mass to a co-linear apparent resistivity measurement is covered by Taylor and Flemming (1988). Of significance here, when considering the polar diagrams, is the fact that the true resistivity parallel to the strike of the fractures is equal to the apparent resistivity measured normal to strike. This is known as the paradox of anisotropy (Keller and Frischknecht, 1966).

Data were collected using the Offset Wenner array (Barker 1981) at an azimuthal increment of 15°. The Offset Wenner array is particularly applicable because the two offset data sets provide an indication of the significance of lateral effects. In the subsequent polar diagrams these two data sets are refered to as D1 and D2. The variation due to lateral effects must be smaller than the variation due to anisotropy before a fracture azimuth can be recognised.

3.2 Detailed apparent resistivity measurements

These data were taken with the dipole-dipole array which utilises in-line, but separated potential and current dipoles. The depth of investigation is increased by moving the dipoles apart in integer increments of the dipole length. The dipole length was 2 m, hence data were collected with the dipoles separated from 2 to 12 m (6 measurements corresponding to n = 1 to 6). Data are plotted at the mid point between the dipoles with the plotting depth from the surface increasing with increasing dipole separation.

These data were collected with the BGS developed resistivity equipment known as RESCAN. The equipment is a computer controlled, multiple electrode system which leads to rapid collection of large data sets. It also allows the operator to monitor the measured voltage waveform and, hence, assess data quality.

Interpretation has been carried out with commercial inversion software, RES2DECO. From the plotted pseudosection of collected data this creates a two dimensional earth cross section of resistivity. These intrinsic resistivities can then be related to the geological section from a knowledge of the intrinsic resistivities gained from the apparent resistivity soundings.

3.3 Apparent resistivity soundings

For a sounding the current electrodes are expanded outwards from a central point to produce a resistivity (inverse of conductivity) sounding which indicates the change in electrical structure of the ground with depth. Data were taken with an ABEM Terrameter and the electrodes were configured in the Schlumberger array. In order to explore the shallow sub-surface, the current electrodes were expanded from an initial separation of 1 m at a logarithmic interval which produces ten measurements per log decade.

Apparent resistivity data are interpreted in terms of a one dimensional horizontally stratified earth. The software used is in-house to the BGS but utilises the linear filter method due to Johansen (1975). One dimensional interpretations are not unique as there are a range of layer resistivities and thicknesses that can produce equivalent models.

4. Presentation of results

The locations at which data were collected are shown in Figure 1. All of the sites are on till except for the sounding and azimuthal data taken at site 4 which is on chalk. In Figure 1 the locations are refered to by method and site (or RESCAN line No.). The methods are S, A and R for soundings, azimuthal measurements and RESCAN dipole-dipole measurements respectively, while sites range from 1 to 6 and RESCAN lines from 1 to 8.

4.1 Apparent resistivity soundings

Soundings were undertaken to provide some estimates of the intrinsic resistivities of the lithologies and to provide some estimates of the thickness of the till. All soundings were made with the Schlumberger array with the current electrode separation (AB) expanding from 1.0 to 200 m in increments of 1/10 th of a log decade.

Sounding 4 was taken on the chalk and was undertaken in order that the presence of the chalk would be recognised in the other data sets. The interpretation in Figure 2 indicates thin near surface resistive layers which probably indicate soil and cover sand. These are underlain by a 70 ohm.m layer (weathered chalk) and a chalk sub-stratum (85 ohm.m). This is a low resistivity for chalk and suggests that the chalk is highly fractured.

Sounding 1 was obtained along the resistive feature identified by Hopson and Morigi (1993). Since this feature only has a limited west to east extent an interpretation of the upper sand layer in terms of a layered model is likely to be approximate. The interpretation in Figure 3 consists of an upper sand layer over two conductive units (32 and 27 ohm.m) which are tentatively interpreted as fractured and less fractured till respectively. The chalk sub-stratum (76 ohm.m) is at a depth of 11.0 m.

Sounding 2 was obtained some 150 m east of sounding 1 in an area where the ground conductivity data (Hopson and Morigi, 1993) were consistently conductive indicating till under no appreciable thickness of cover sand. The interpretation (Figure 4) indicates conductive till (24 ohm.m) beneath a soil layer with no splitting of the till layer. The chalk (65 ohm.m) is again at a depth of 11.0 m.

Sounding 3 was to the west of the Harling Road and produced the poorest quality sounding curve, possibly due to the near-by presence of a water pipe. The interpretation in Figure 5 is very similar to that for sounding 2, but with an interpreted depth to chalk of 15.0 m.

4.2 Azimuthal apparent resistivity

Data were taken initially at site 4 on the chalk so that any underlying fracture trends in the chalk would be recognised in the data taken at till sites. The results are shown in Figure 6. At the smallest electrode separation of 2 m an azimuthal trend of 105° is shown and at a = 8 m two poorly defined fracture trends of 120° and 190° are indicated. At the two largest electrode separations high apparent resistivities were measured at an azimuth of 120°, the cause of which is unknown. The data at these two sites are also shown with the data from an azimuth 120° removed. The result is that no other azimuthal trends other than those already described are observed. These data thus indicate that there may a fracture set in the chalk at an orientation of 105°, but the fracture length must be small since it is not observed in data taken at larger electrode separations. Alternatively since the electrode array spacing was small this feature may be related to the soil and sand overburden. This is in contrast to other azimuthal data taken on the chalk (Busby and Peart, 1994) where fracture sets of long fracture length were observed.

The remaining azimuthal data sets were all taken at till sites and are shown as follows; Figure 7 is site 1, Figure 8 is site 2 the most easterly site, Figure 9 is site 5, adjacent to the BGS borehole array and Figure 10 is site 6 the most southerly site. There are very few azimuthal trends in these data given that the variation due to lateral effects (deviations between the D1 and D2 data sets) must be less than the azimuthal variation. The only consistent trends are seen in the a = 16 and 32 m data from site 5 (Figure 9) which shows a possible fracture orientation of 210° and from site 6 (Figure 10) at a spacing of a = 16 m which shows a peak at an orientation of 225°. Given that the azimuthal increment was 15° this is probably the same orientation at the two sites.

Percentage anisotropy values and average resistivities for the observed azimuthal variations are shown below.

	Site 5 a = 16 m	Site 5 a = 32 m	Site 6 a = 16 m
% anisotropy	± 6 %	± 6 %	± 3 %
Av. value	37 Ωm	50 Ωm	38 Ωm

These display low values for the anisotropy. The same apparent resistivity values obtained for a = 16 m at sites 5 and 6 indicate that the same geological sequence was under investigation. The reduction in percentage anisotropy between the two sites suggests a reduction in fracture intensity from site 5 to site 6. The increased apparent resistivity at a = 32 m indicates the increased influence of the underlying chalk.

The lack of observed peaks in the polar diagrams either indicates a lack of fracture sets with a preferred orientation in the till or a lack of resistivity contrast between the fractures and the conductive till.

4.3 Detailed apparent resistivity measurements

The locations of the eight lines of detailed dipole-dipole apparent resistivity data are shown in Figure 1 (R1 - R8). These data were collected as overlapping spreads where each spread was 78 m long. A sketch detailing the spread layout and the co-ordinate system used to define the layout is shown in Figure 11. The lines are approximately normal to the resistive feature identified by Hopson and Morigi (1993). An initial interpretation of this feature is that it represents a thickening sequence of resistive cover sand over conductive till. Sounding S1 along the feature indicated that the sand has a resistivity of around 200 ohm.m compared to 30 ohm.m for the till.

Pseudosections of apparent resistivity (in ohm.m) for the eight surveyed lines are shown in Figures 12 to 14. Blank areas are due to poor data quality. The scale, marked as 'Depth' is a pseudodepth and not a true depth. The sections clearly define a resistive surface layer (sand) over a conductive sub-stratum (till). The eastern edge of the sand displays a slight westerly trend between lines, up to line 8. The western edge extends beyond the survey on many of the lines. Depths are indicated to be a few metres and there is some suggestion of a mixing of till and sand (or increased quantities of glacial sand within the till) on lines 3 and 5.

Interpretation has been carried out with the inversion software RES2DECO. Due to programme limitations each spread has been interpreted separately. Results for each spread are presented as plots of apparent resistivity, calculated apparent resistivity and the model where a common resistivity scale is used throughout. In the models low resistivities (blue to green areas) represent till whilst higher resistivities (yellow to red areas) represent sand. No interpretation is presented for spread 1 due to the quantity of poor data. The results for the remaining spreads (2 - 17) are shown in Figures 15 to 30.

Figure 31 is a contour plot of the depth to the base of the surface sand layer, which summarises the interpretation. The sand to till interface has been selected as the 75 ohm.m contour in the model plots. This is a lower value for sand than indicated by the sounding, but there is likely to be a mixing layer. There is no contour for 0.5 m depth as the minimum depth resolved by the inversion is 0.45 m. Hence the location of the 0 m contour is approximate and the entire area could be covered by up to 0.45 m of sand. The plot defines a north trending sand channel with a thickening at the western ends of lines 3 and 4. Maximum depth of sand is 2 m. A small sand body is located at the eastern ends of lines 2 and 3 of depth up to 1.5 m.

5. Conclusions

The apparent resistivity soundings have generated consistent intrinsic resistivities for the strata encountered. These are 100 - 200 ohm.m for cover sand, 22 - 32 ohm.m for till and 65 - 85 ohm.m for chalk. At the sounding sites, interpreted depths to the chalk range from 11 to 15 m.

The azimuthal apparent resistivity measurements displayed few trends. No significant fracture sets were identified within the chalk. An orientation of 105° recognised in the data taken at the smallest electrode separation may be related to the soil and cover sand. The low resistivities obtained for the chalk indicate that it is highly fractured. Only at sites 5 and 6 was a fracture trend tentatively recognised within the till. This occurs at an azimuth of 210° - 225° and there is an indication that the degree of fracturing decreases from site 5 to site 6. The lack of fracture orientations recognised within the till may indicate either a lack of uniform fracturing or that a sufficient resistivity contrast is not developed between the fractures and the till so that the till does not behave anisotropically (in a resistive sense).

The detailed dipole-dipole apparent resistivity data have clearly identified the resistive sand overlying the conductive till. Interpretation of the data indicates a northerly trending sand channel with maximum depths of up to 2 m. A number of thickenings and shallowings are recognised and a small sand body, with a depth of up to 1.5 m occurs at the eastern end of lines 2 and 3.

6. References

Barker R D, 1981. The Offset Wenner system of electrical resistivity sounding and its use with a multicore cable. Geophysical Prospecting, v. 29, pp. 128-43.

Busby J P and Peart R J, 1994. Azimuthal resistivity and seismic measurements for the determination of fracture orientations. In: Preprints of papers; Modern Geophysics in Engineering Geology (eds. D M McCann, P Fenning, J Cripps), The Engineering Group of the Geological Society, pp. 205-216.

Hopson P M and Morigi A N, 1993. Hydrogeological classification of superficial clays: Report on the detailed field mapping to characterise the till in the Elmdon, Essex and Garboldisham, Norfolk pilot study areas.

Johansen H K, 1975. An interactive computer-graphic-display-terminal system for interpretation of resistivity soundings, Geophysical Prospecting, v. 23, p. 449.

Keller G V and Frischknecht F C, 1966. Electrical methods in Geophysical Prospecting. Pergamon Press, New York. 519 p.

Taylor R W and Fleming A H, 1988. Characterizing jointed systems by azimuthal resistivity surveys. Ground Water, v. 26, No. 4, pp. 464-74.

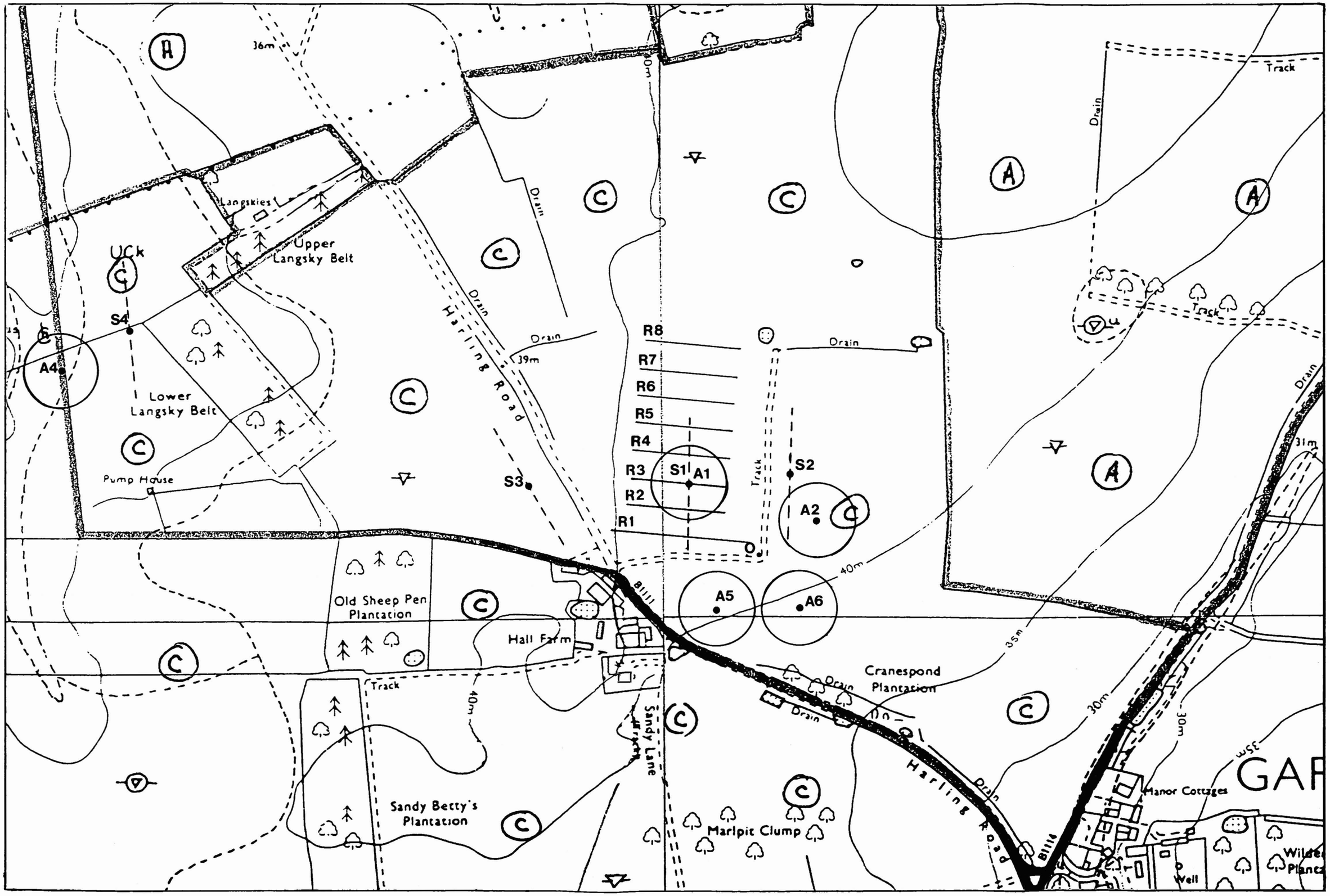

Figure 1. Location of apparent resistivity measurements at the Garboldisham pilot study area in Norfolk. Soundings (1 to 4) are denoted by S, azimuthal measurements (1,2,4,5 and 6) by A and RESCAN detailed dipole-dipole measurements (1 to 8) by R. The origin of the grid for the RESCAN survey lines is denoted by O. Note the RESCAN lines are approximately normal to the resistive feature identified by Hopson and Morigi (1993). Scale 1:5000 from original topographic base at 1:10000.

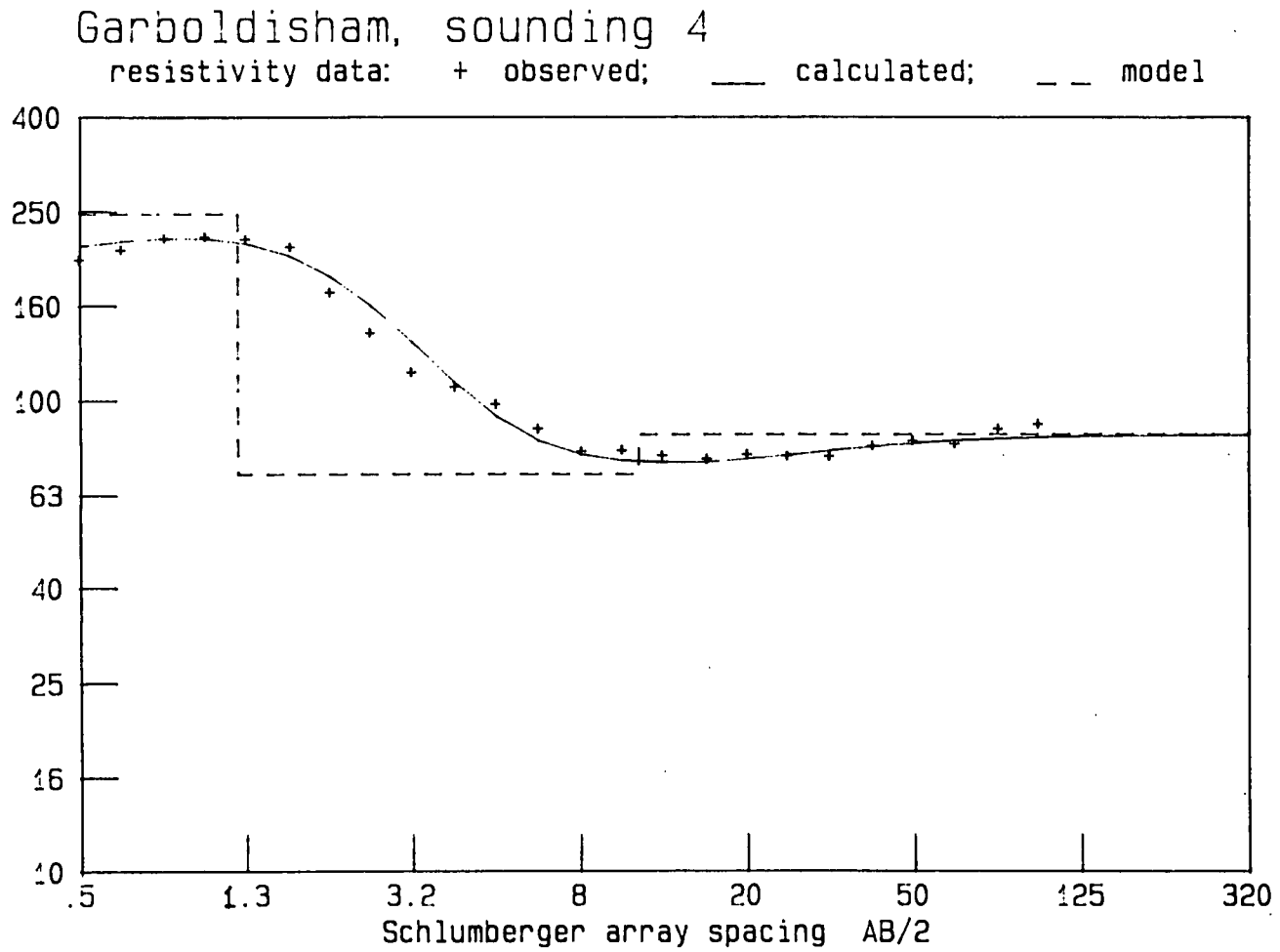

Garboldisham, sounding 4

Layer	Thickns.	Restvty.	Depth
1	0.20	190.00	0.20
2	1.00	250.00	1.20
3	9.80	70.00	11.00
Substrait		85.00	******

Figure 2. Resistivity sounding and interpretation from site 4, located on exposed chalk.

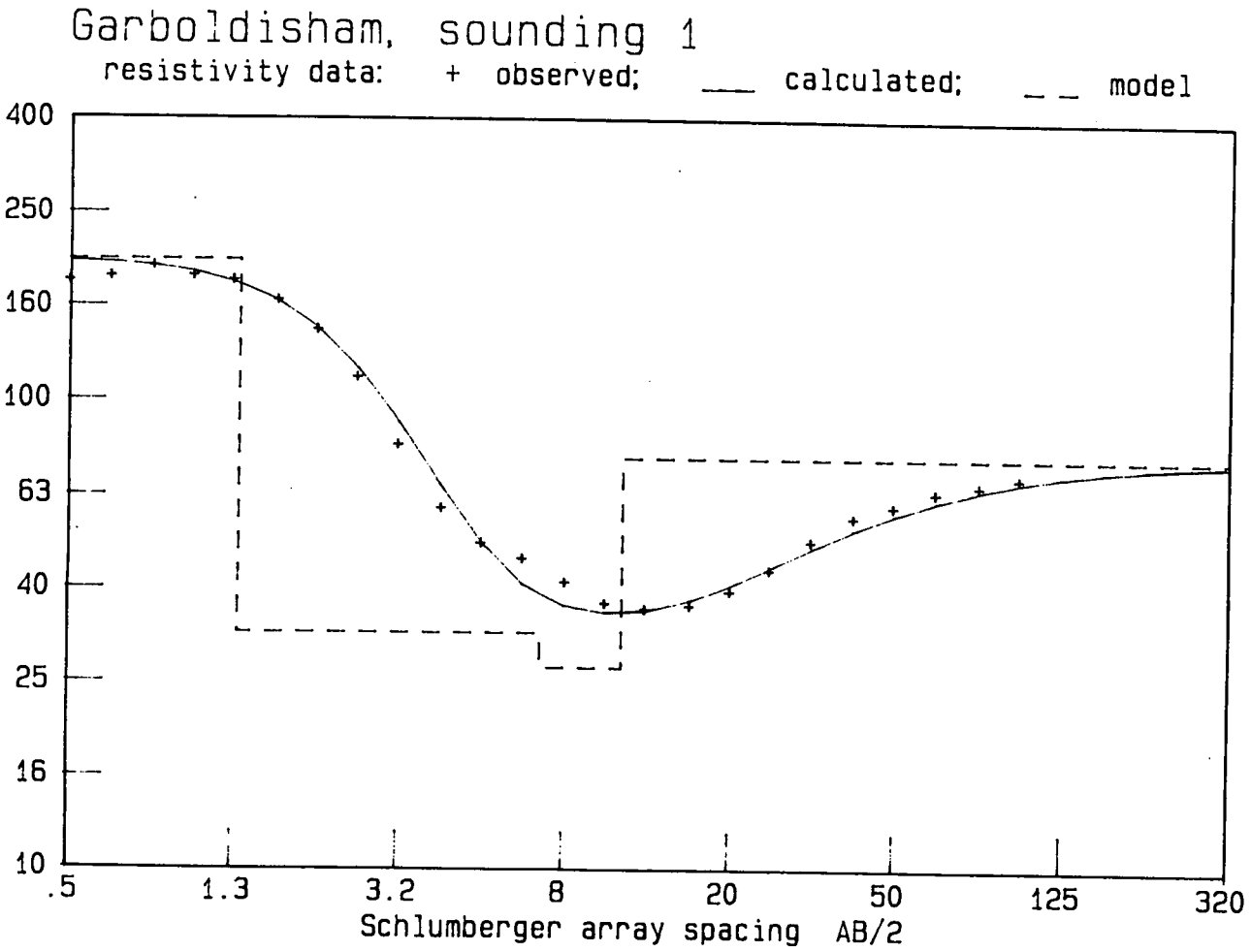

Garboldisham, sounding 1

Layer	Thickns.	Restvty.	Depth
1	1.30	200.00	1.30
2	5.70	32.00	7.00
3	4.00	27.00	11.00
Substrait		76.00	******

Figure 3. Resistivity sounding and interpretation from site 1.

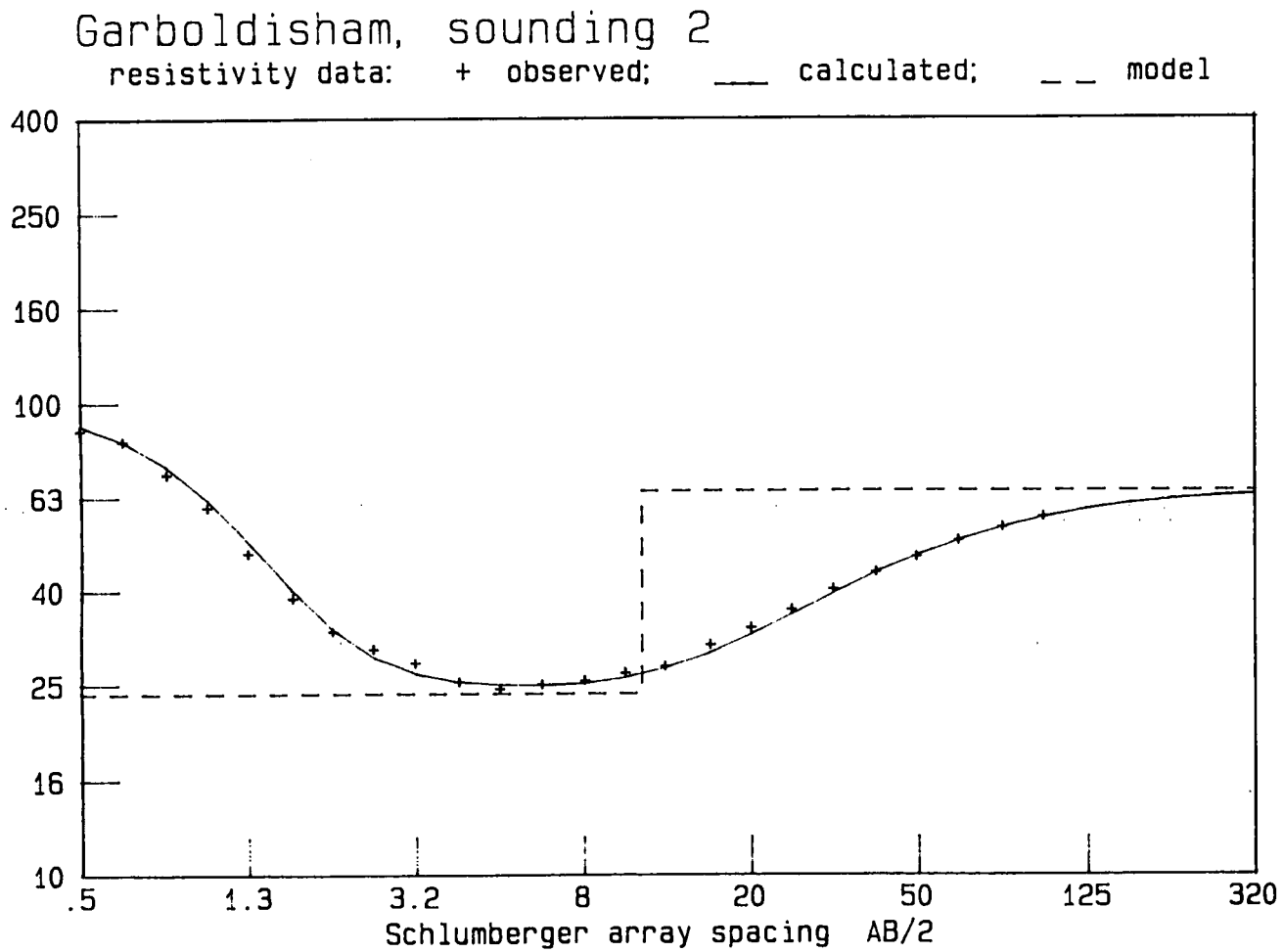

Garboldisham, sounding 2

Layer	Thickns.	Restvty.	Depth
1	0.50	100.00	0.50
2	10.50	24.00	11.00
Substrait		65.00	******

Figure 4. Resistivity sounding and interpretation from site 2.

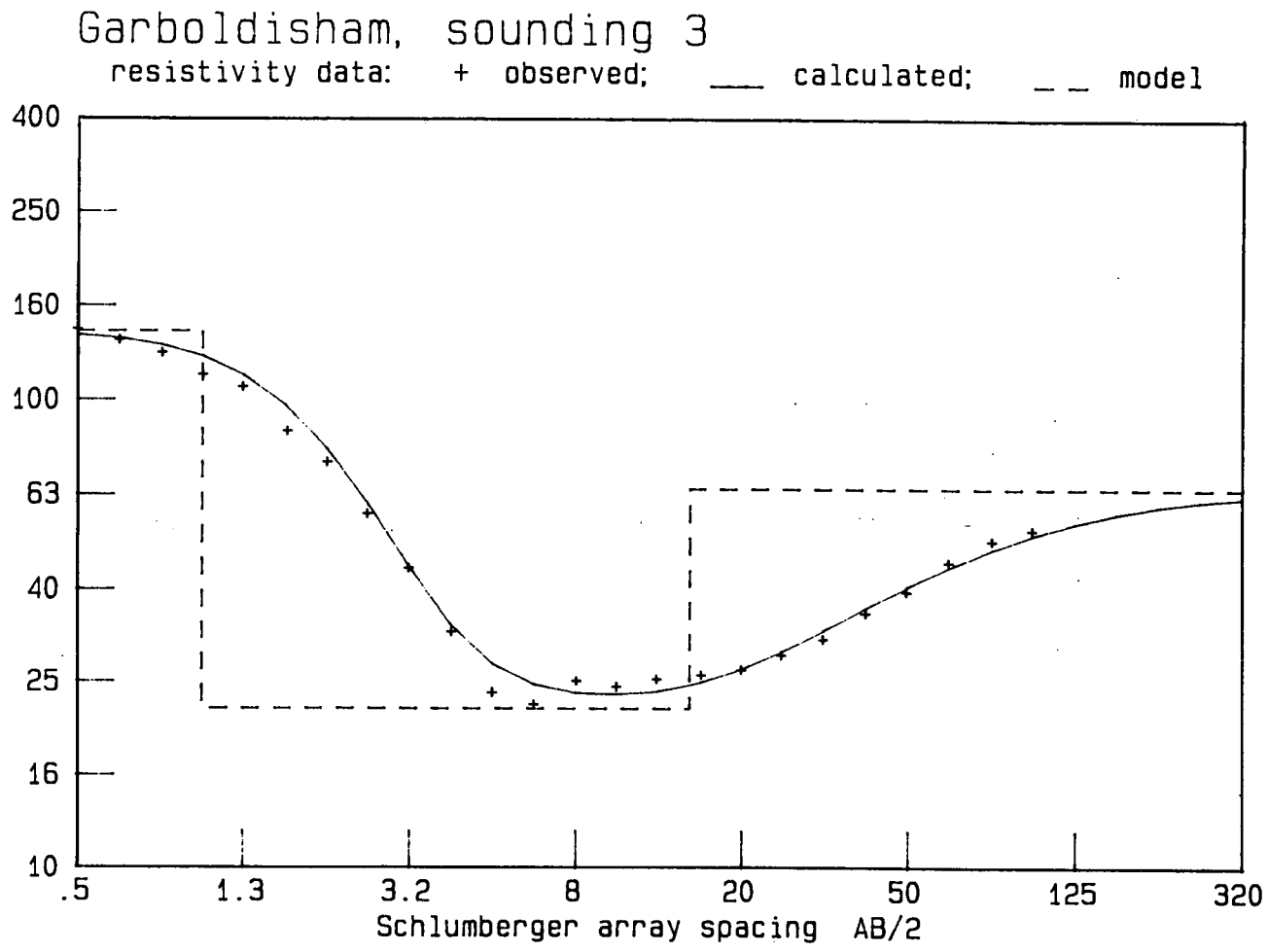

Garboldisham, sounding 3

Layer	Thickns.	Restvty.	Depth
1	1.00	140.00	1.00
2	14.00	22.00	15.00
Substrait		65.00	******

Figure 5. Resistivity sounding and interpretation from site 3.

Garboldisham chalk site (site 4)

Offset Wenner array

Co-ordinates [599.16, 283.37]

..... = D1

..... = D2

——— = D1, D2 average

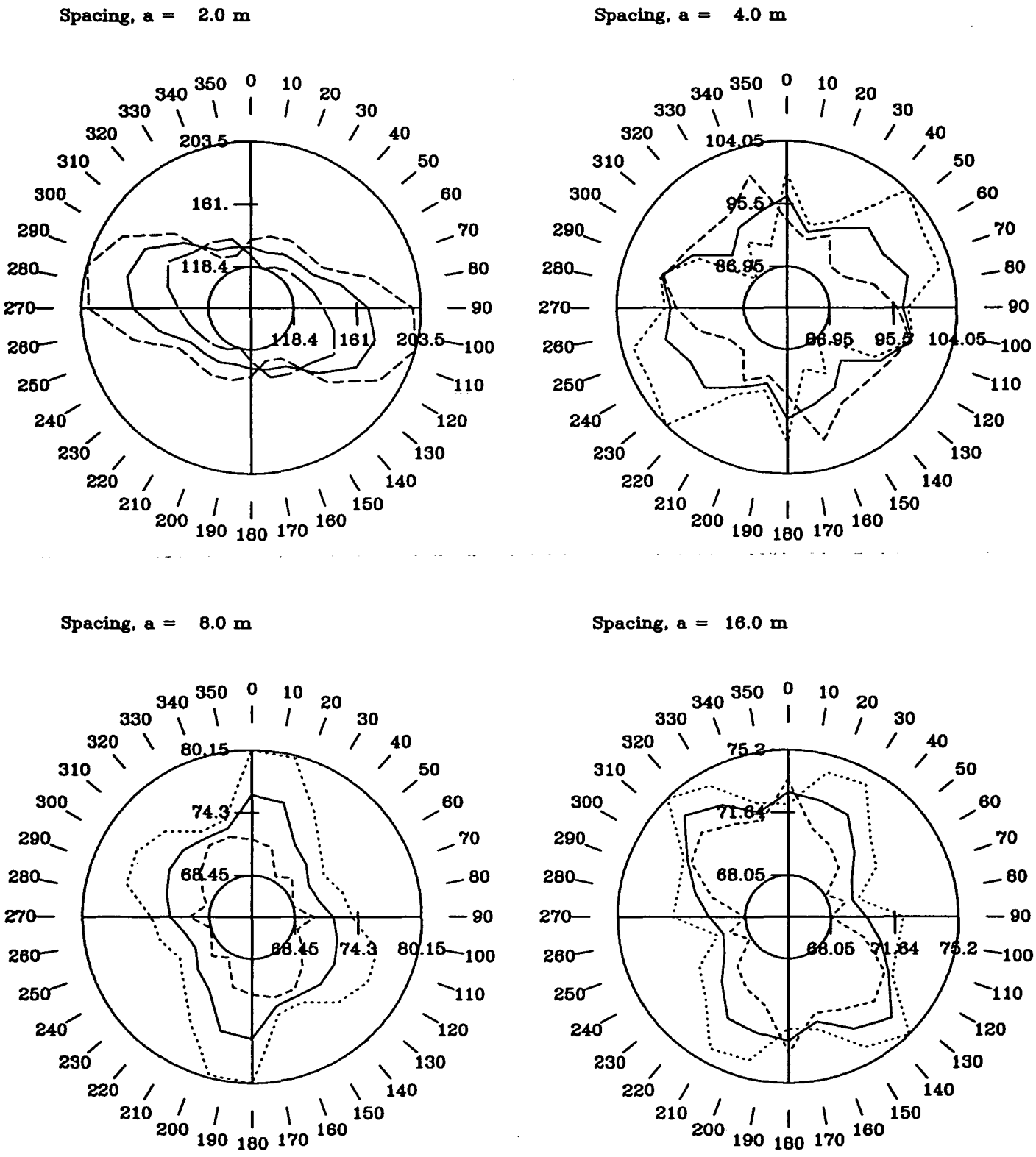

Figure 6a. Polar diagrams of azimuthal apparent resistivity data for electrode array spacings of a = 2 - 16 m from site 4.

Garboldisham chalk site (site 4)

Offset Wenner array

Co-ordinates [599.16, 283.37]

..... = D1

..... = D2

——— = D1, D2 average

Spacing, a = 32.0 m

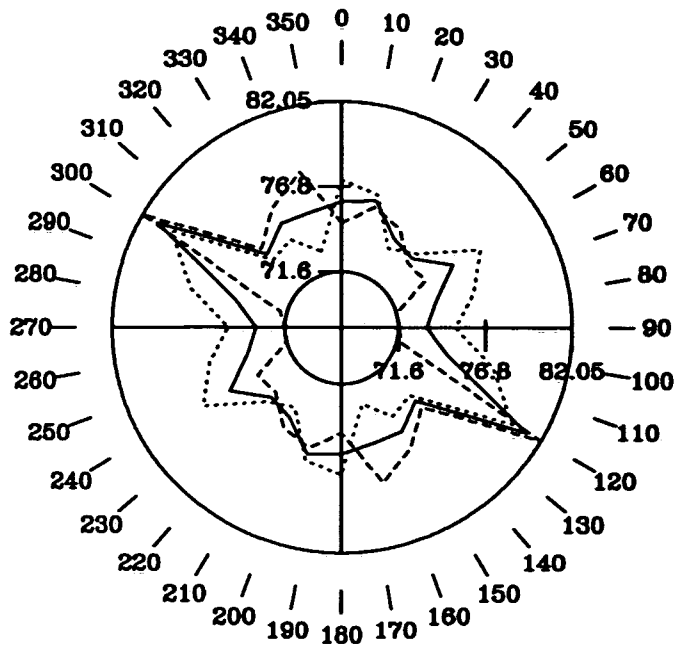

Spacing, a = 64.0 m

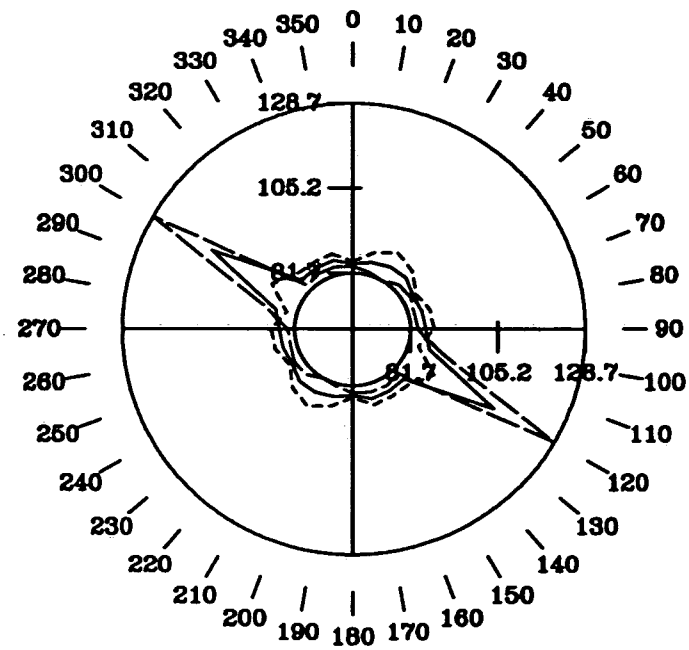

Spacing, a = 32.0 m

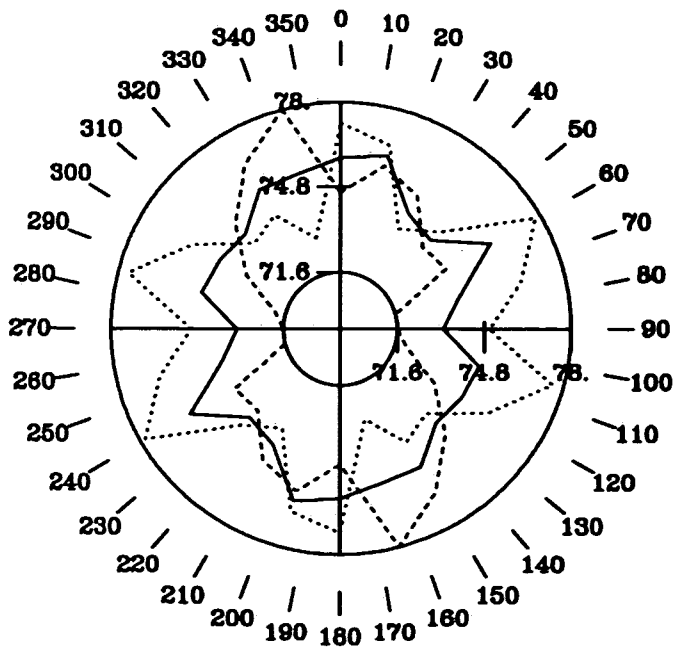

Spacing, a = 64.0 m

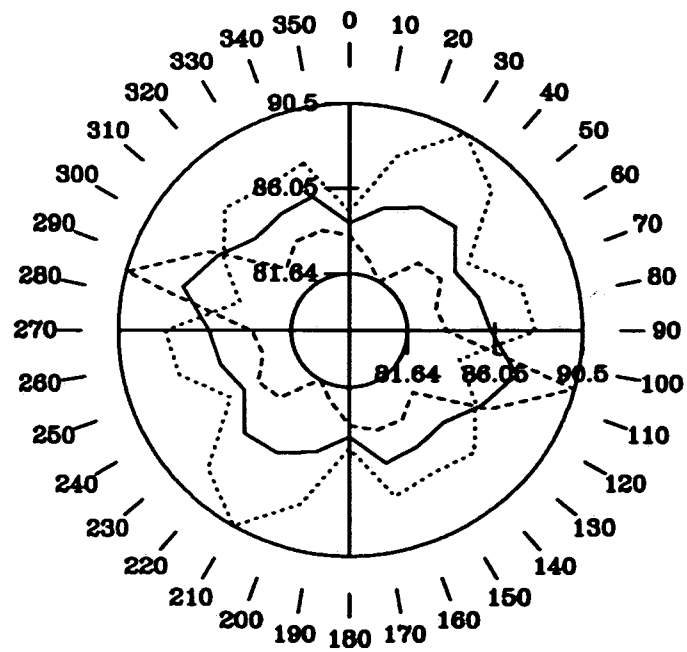

Figure 6b. Polar diagrams of azimuthal apparent resistivity data for electrode array spacings of a = 32 and 64 m from site 4. Note the data are repeated with the value recorded for the azimuth of 120° removed and replaced with an interpolated value.

Garboldisham, resistive feature (site 1)

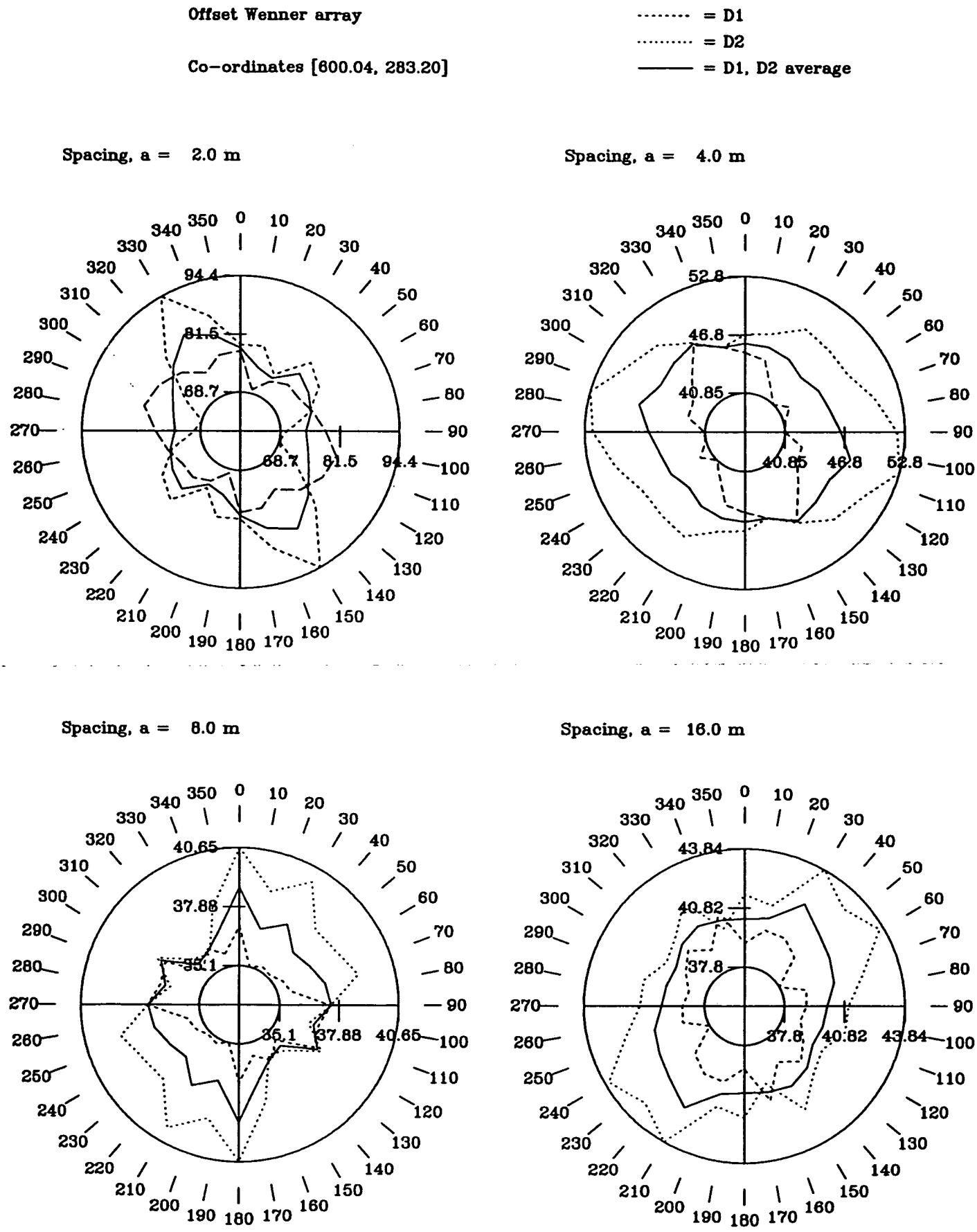

Figure 7a. Polar diagrams of azimuthal apparent resistivity data for electrode array spacings of a = 2 - 16 m from site 1.

Garboldisham, resistive feature (site 1)

Offset Wenner array

Co-ordinates [600.04, 283.20]

..... = D1

..... = D2

——— = D1, D2 average

Spacing, a = 32.0 m

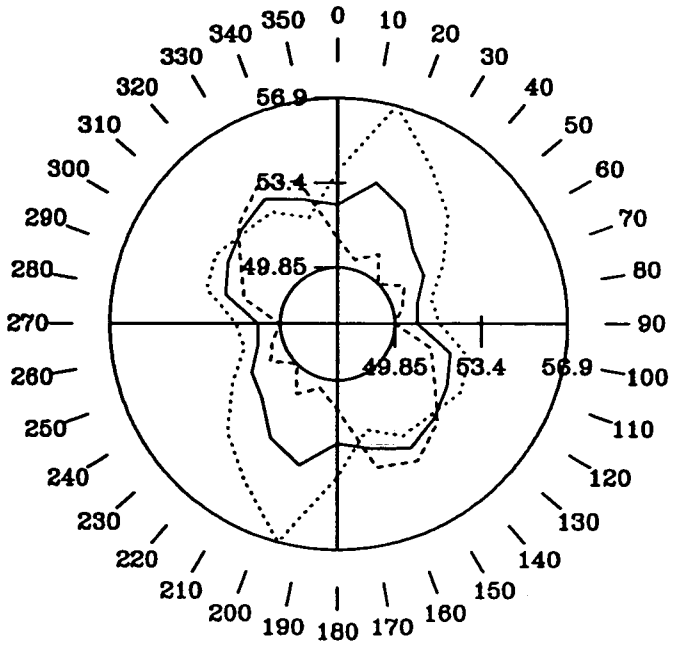

Figure 7b. Polar diagram of azimuthal apparent resistivity data for electrode array spacing of a = 32 m from site 1.

Garboldisham, eastern site (site 2)

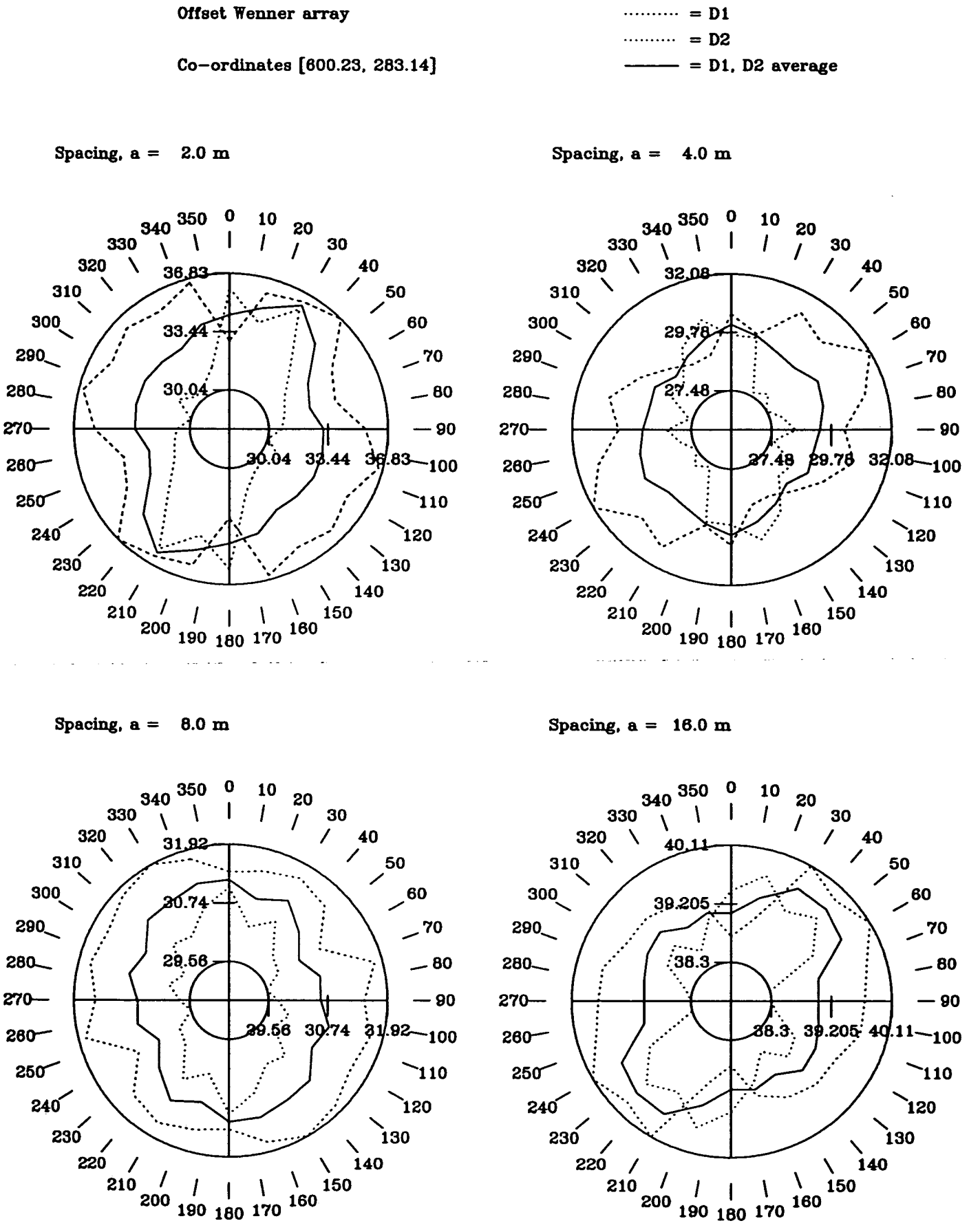

Figure 8a. Polar diagrams of azimuthal apparent resistivity data for electrode array spacings of a = 2 - 16 m from site 2.

Garboldisham, eastern site (site 2)

Offset Wenner array

Co-ordinates [600.23, 283.14]

..... = D1

..... = D2

——— = D1, D2 average

Spacing, a = 32.0 m

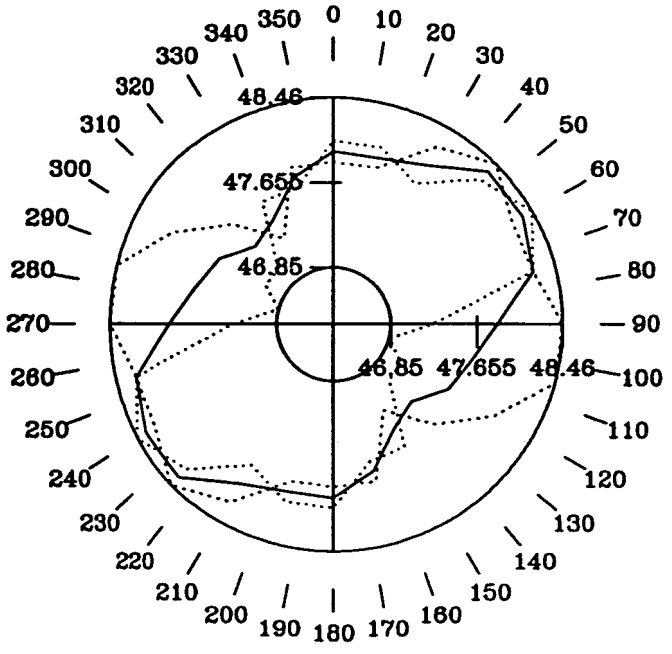

Figure 8b. Polar diagram of azimuthal apparent resistivity data for electrode array spacing of a = 32 m from site 2.

Garboldisham, borehole site (site 5)

Offset Wenner array

Co-ordinates [600.08, 283.01]

..... = D1

..... = D2

——— = D1, D2 average

Spacing, a = 2.0 m

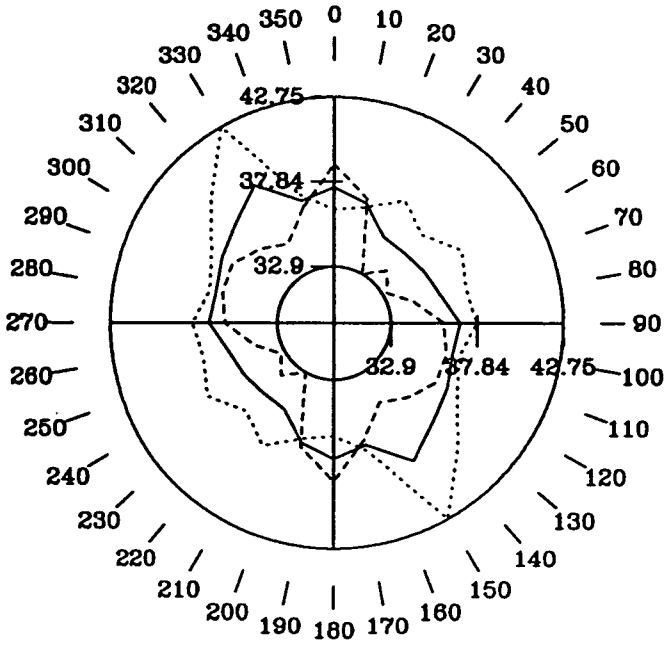

Spacing, a = 4.0 m

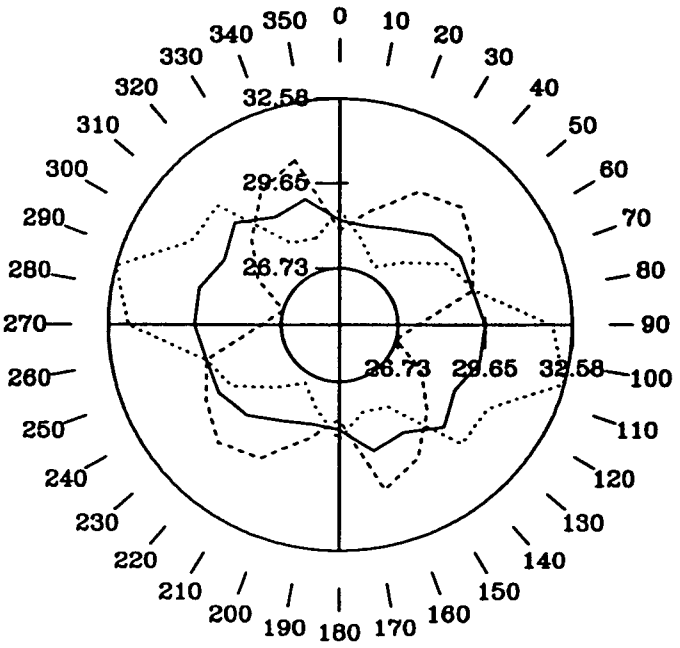

Spacing, a = 8.0 m

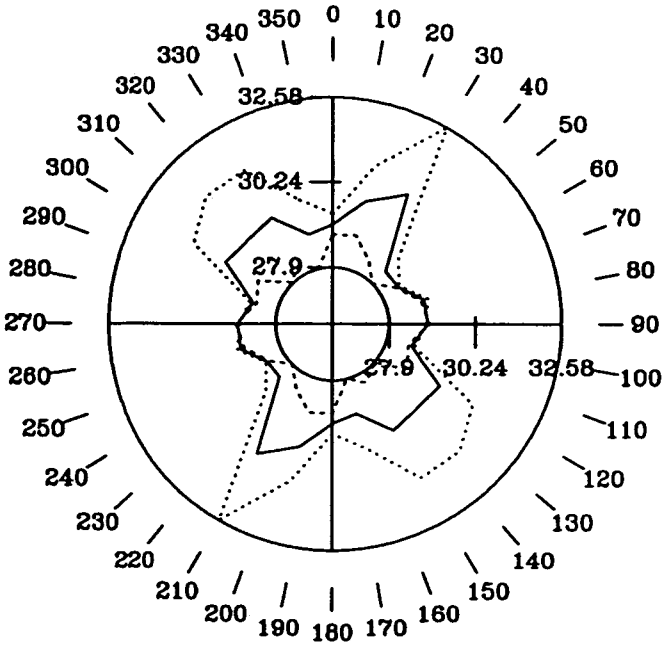

Spacing, a = 16.0 m

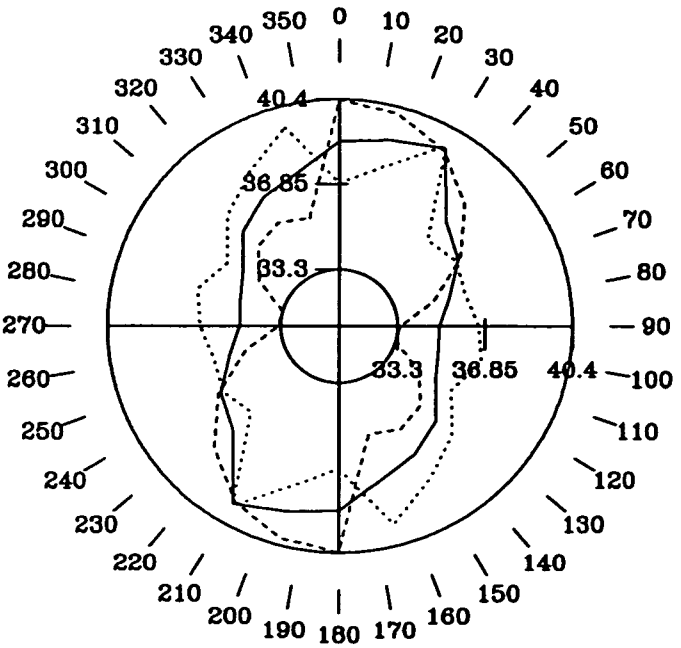

Figure 9a. Polar diagrams of azimuthal apparent resistivity data for electrode array spacings of a = 2 - 16 m from site 5.

Garboldisham, borehole site (site 5)

Offset Wenner array

Co-ordinates [600.08, 283.01]

Spacing, a = 32.0 m

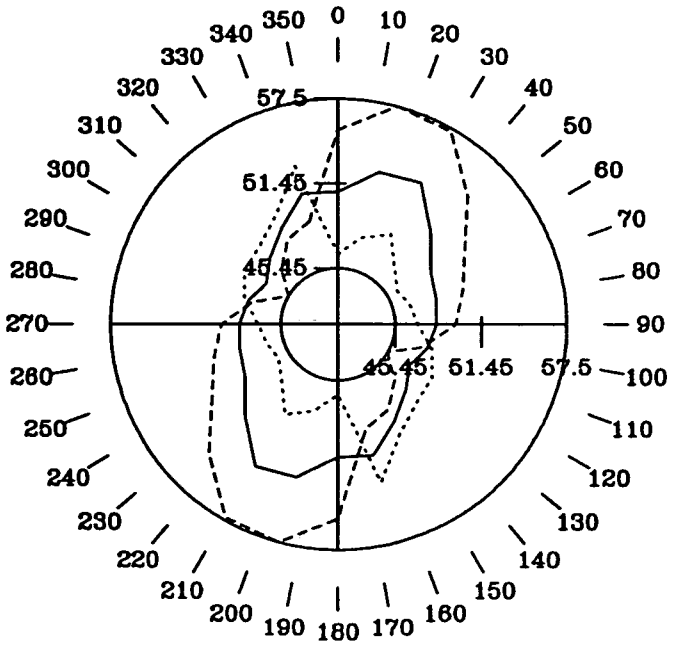

------- = D1

..... = D2

——— = D1, D2 average

Figure 9b. Polar diagram of azimuthal apparent resistivity data for electrode array spacing of a = 32 m from site 5.

Garboldisham, southerly site (site 6)

Offset Wenner array

Co-ordinates [600.20, 283.02]

..... = D1

..... = D2

——— = D1, D2 average

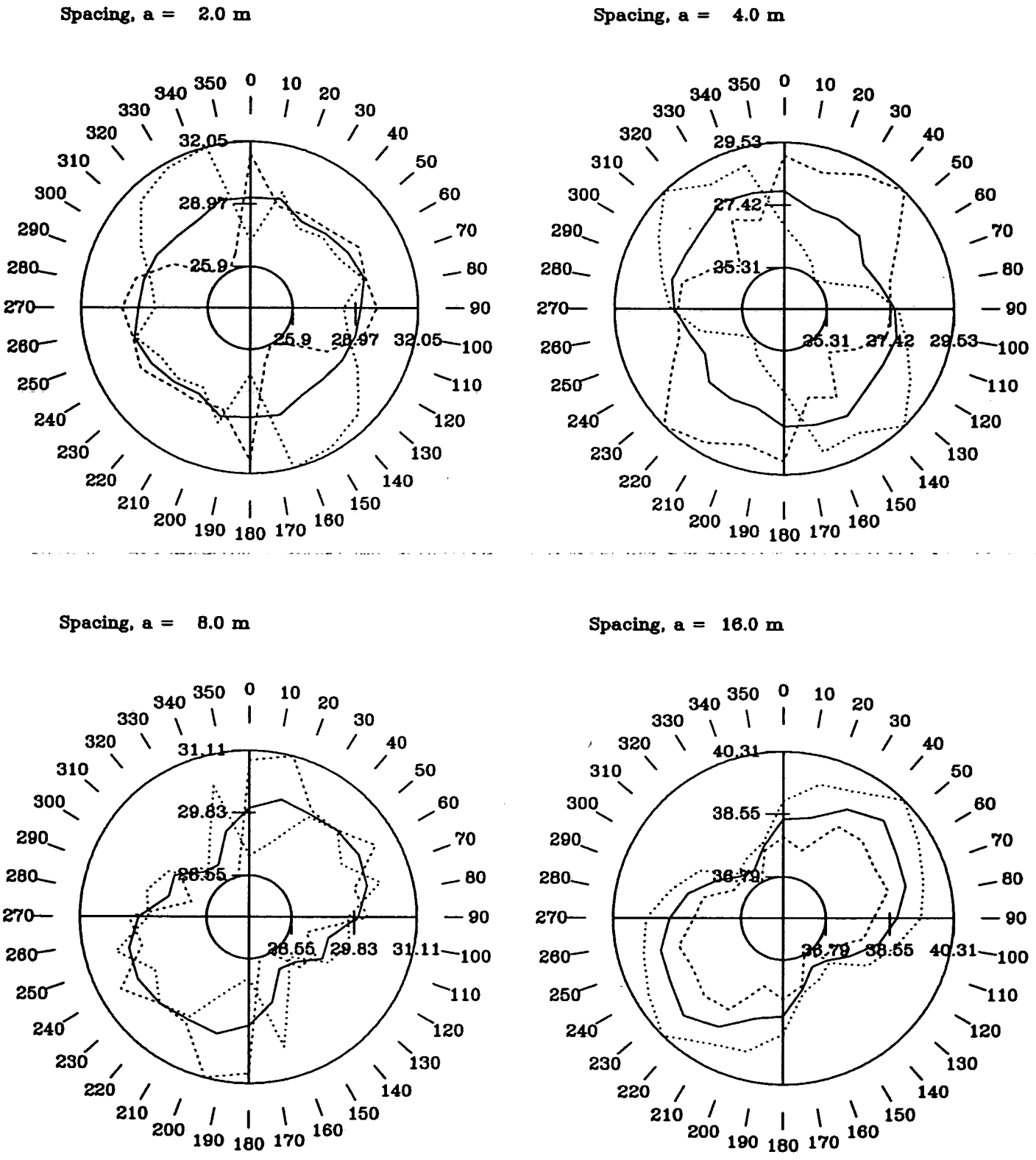

Figure 10a. Polar diagrams of azimuthal apparent resistivity data for electrode array spacings of a = 2 - 16 m from site 6.

Garboldisham, southerly site (site 6)

Offset Wenner array

Co-ordinates [600.20, 283.02]

..... = D1

..... = D2

——— = D1, D2 average

Spacing, a = 32.0 m

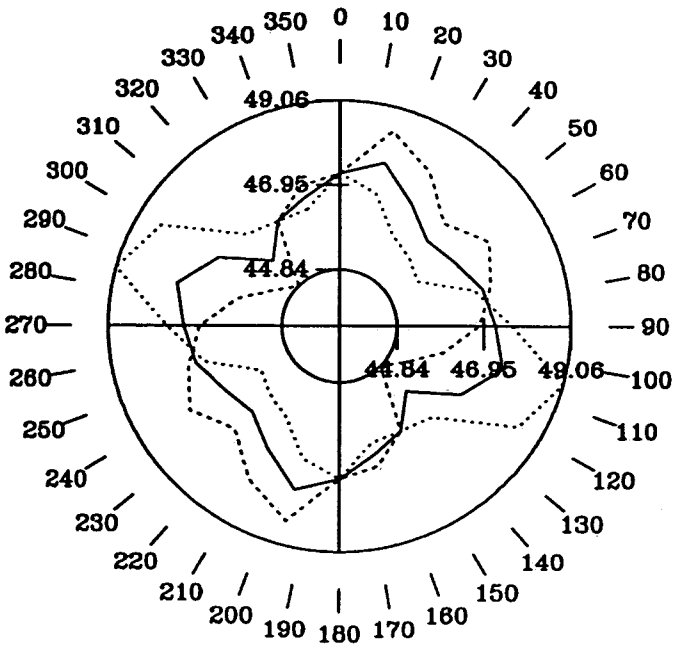

Figure 10b. Polar diagram of azimuthal apparent resistivity data for electrode array spacing of a = 32 m from site 6.

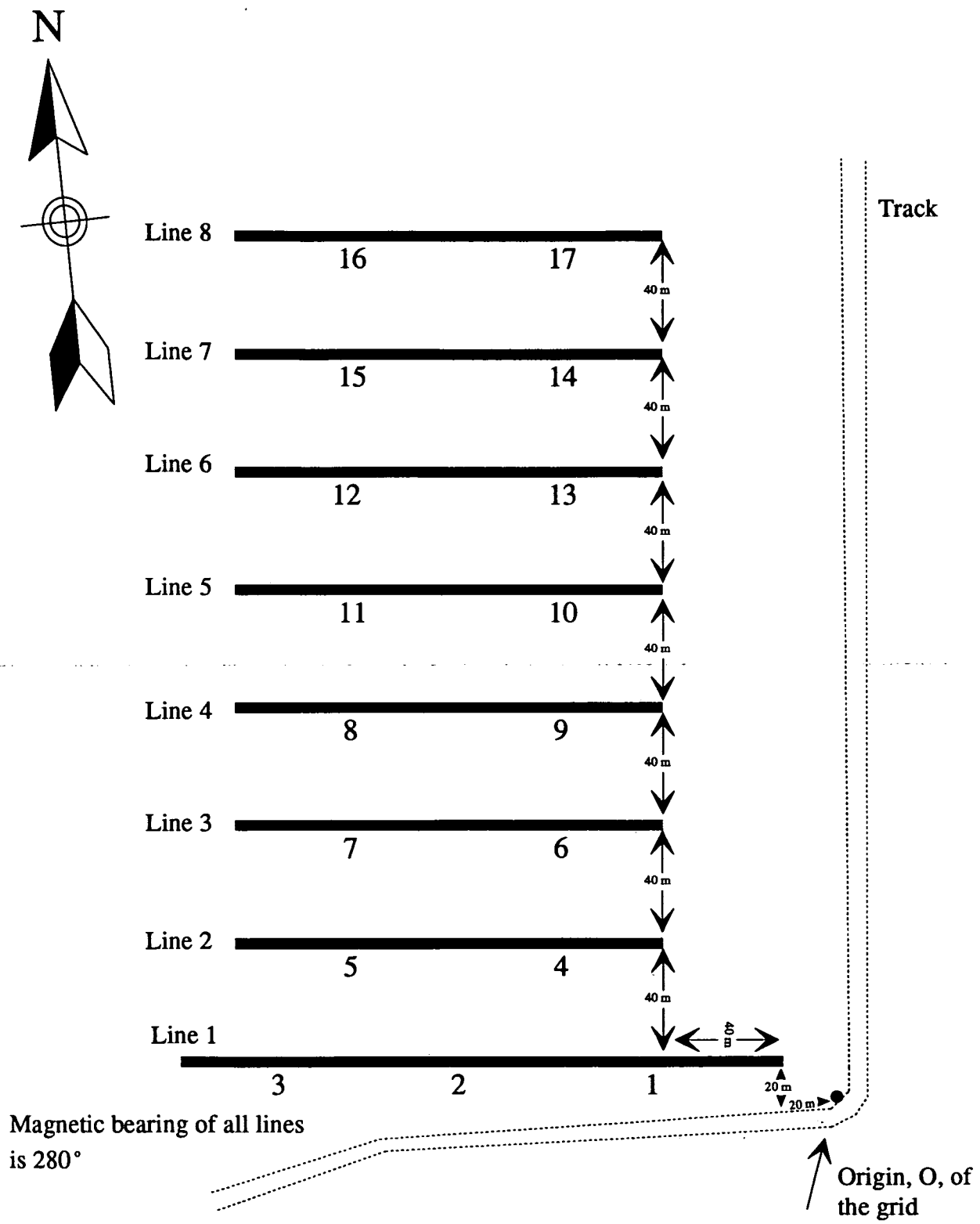

Figure 11. Diagram detailing the spread layout of each of the eight RESCAN lines of detailed apparent resistivity measurements. Each spread (1 - 17) is 78 m long and is orientated from east to west. Grid co-ordinates are relative to the origin O where the positive x axis is parallel to the survey lines and orientated from east to west, the y axis is perpendicular and orientated from south to north.

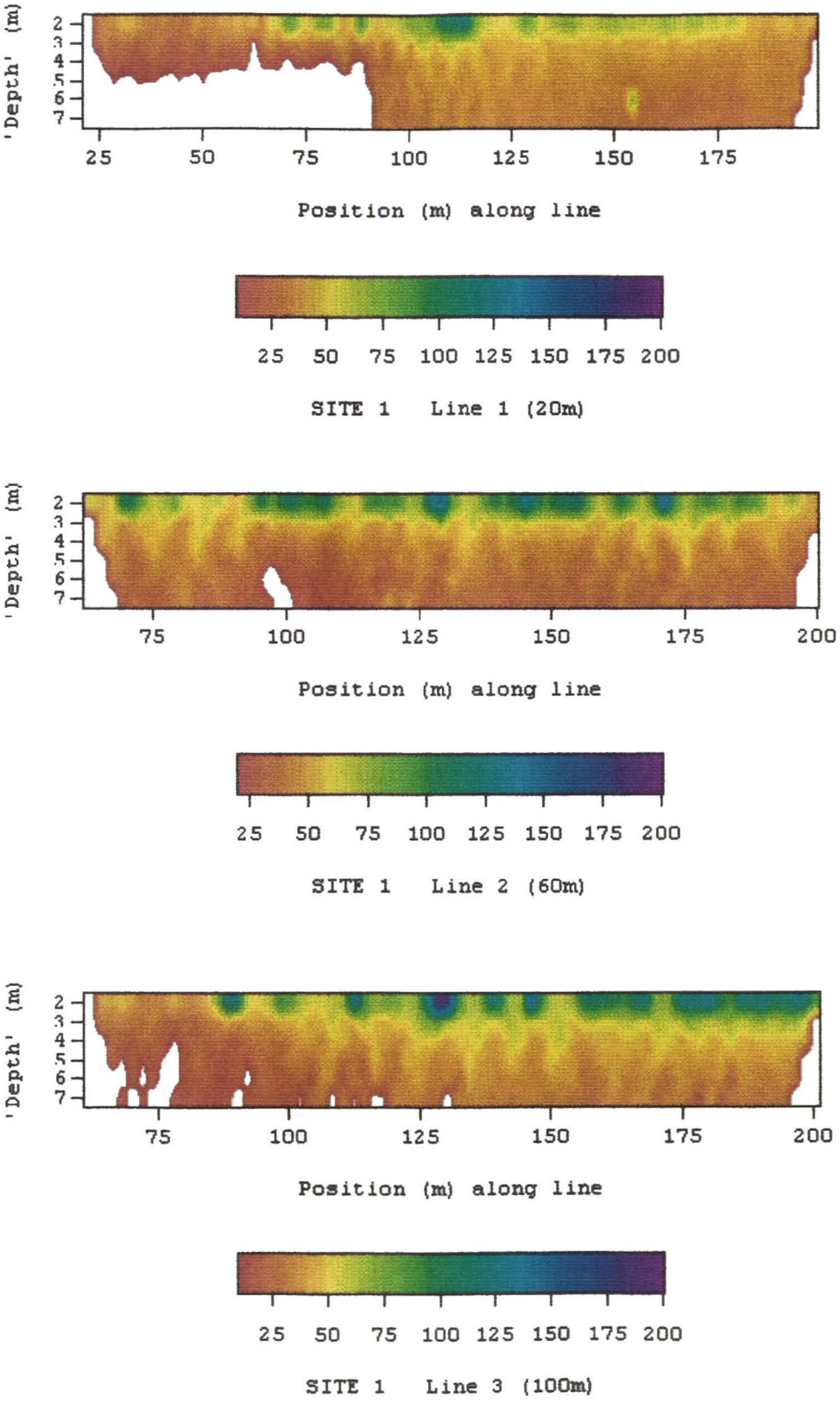

Figure 12. Pseudosections of apparent resistivity (in ohm.m) for lines 1 to 3.

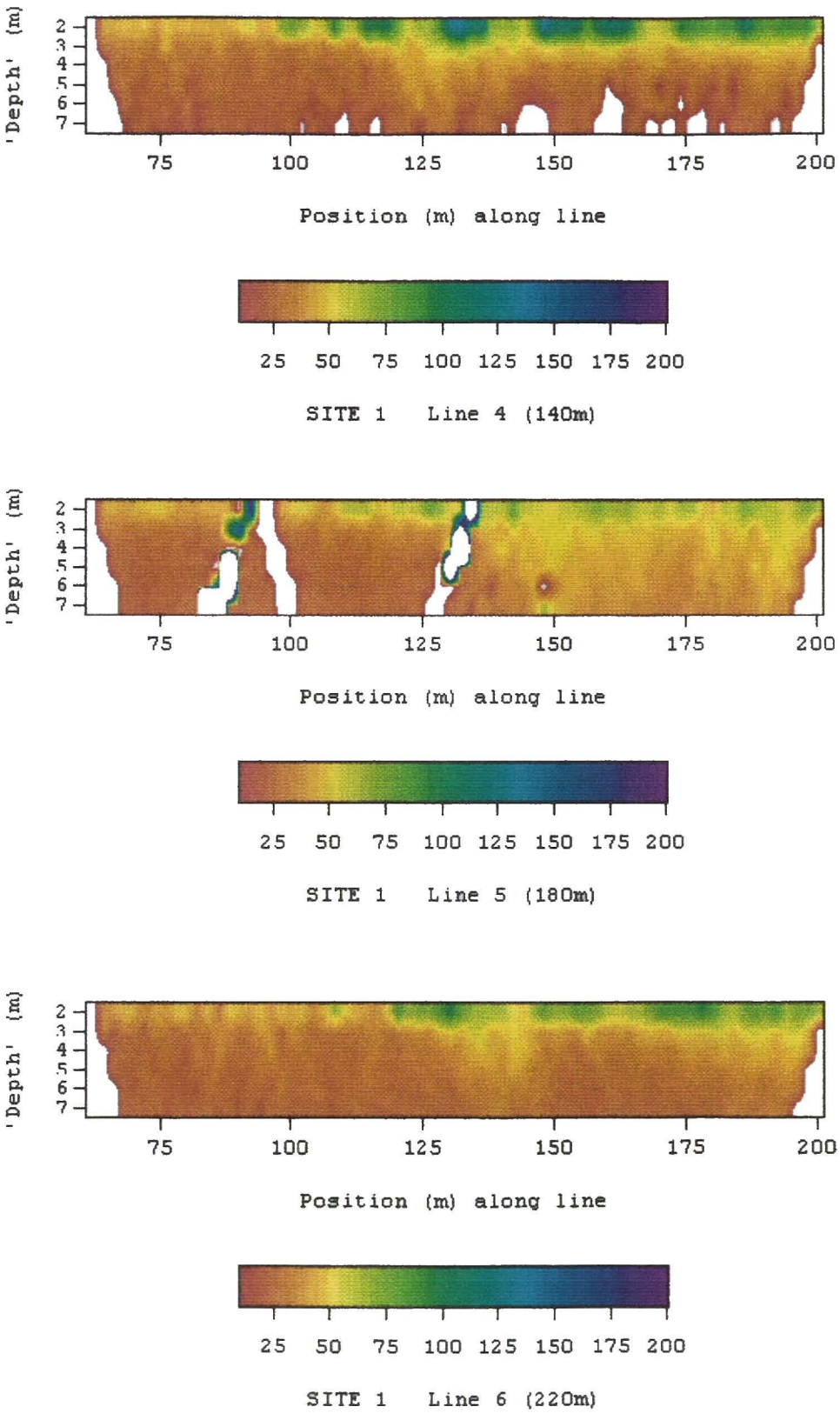

Figure 13. Pseudosections of apparent resistivity (in ohm.m) for lines 4 to 6.

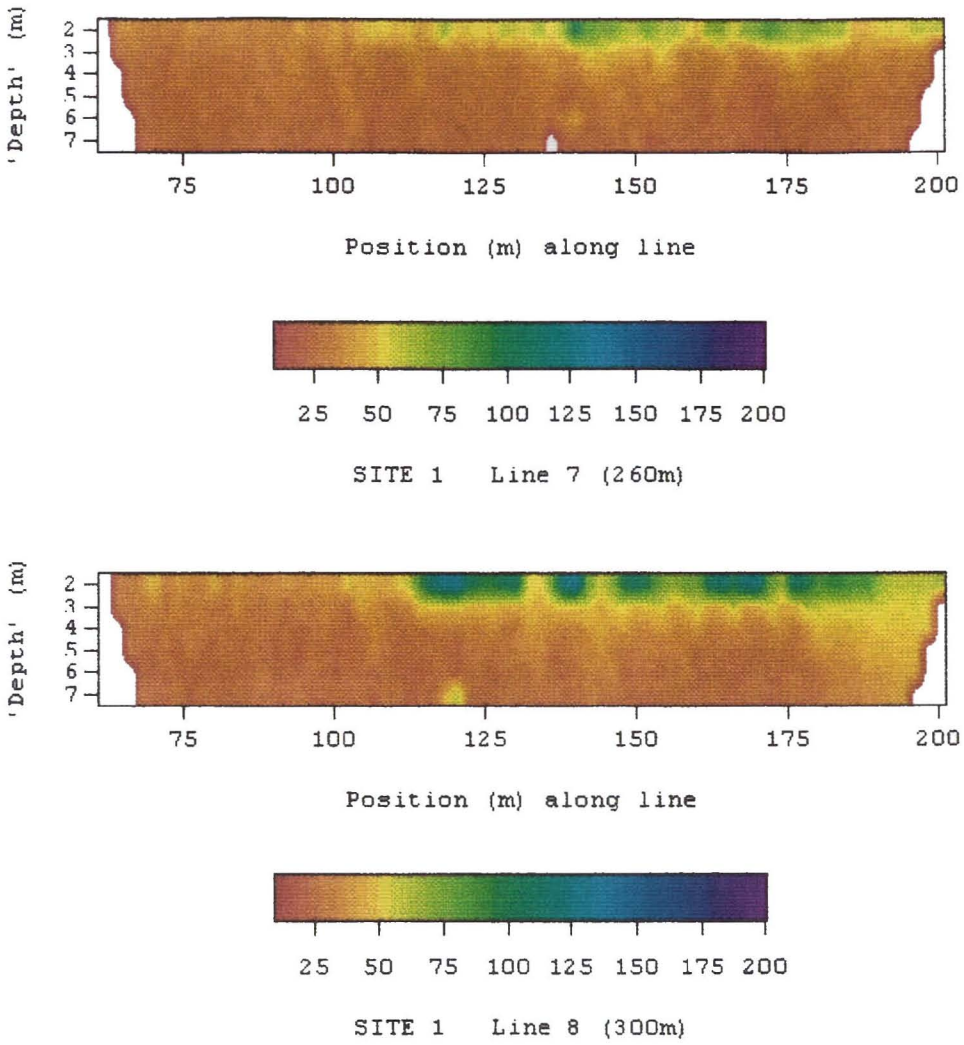

Figure 14. Pseudosections of apparent resistivity (in ohm.m) for lines 7 and 8.

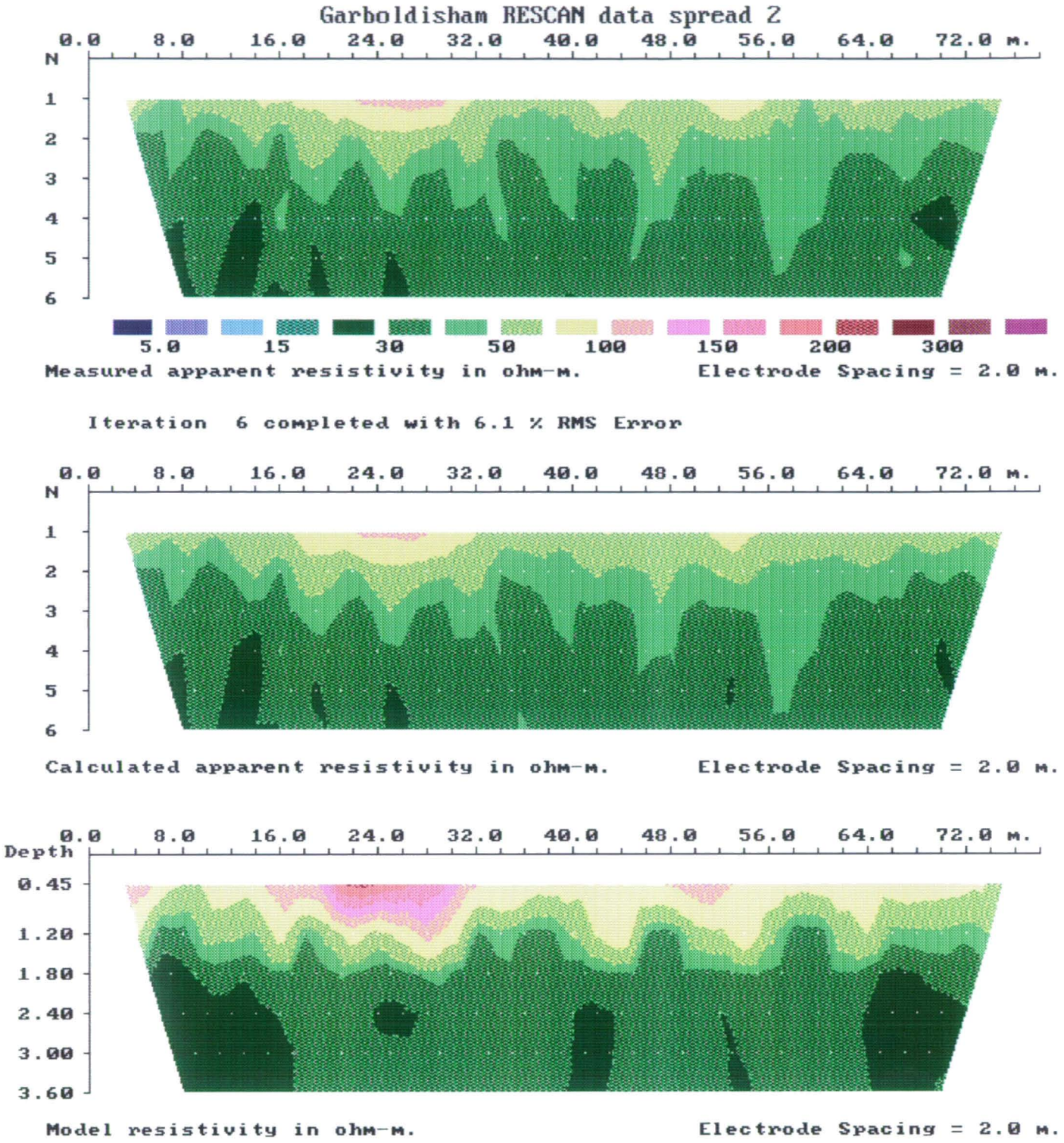

Figure 15. Interpretation results for RESCAN detailed dipole-dipole apparent resistivity measurements, spread 2 (84 - 162 m along line 1).

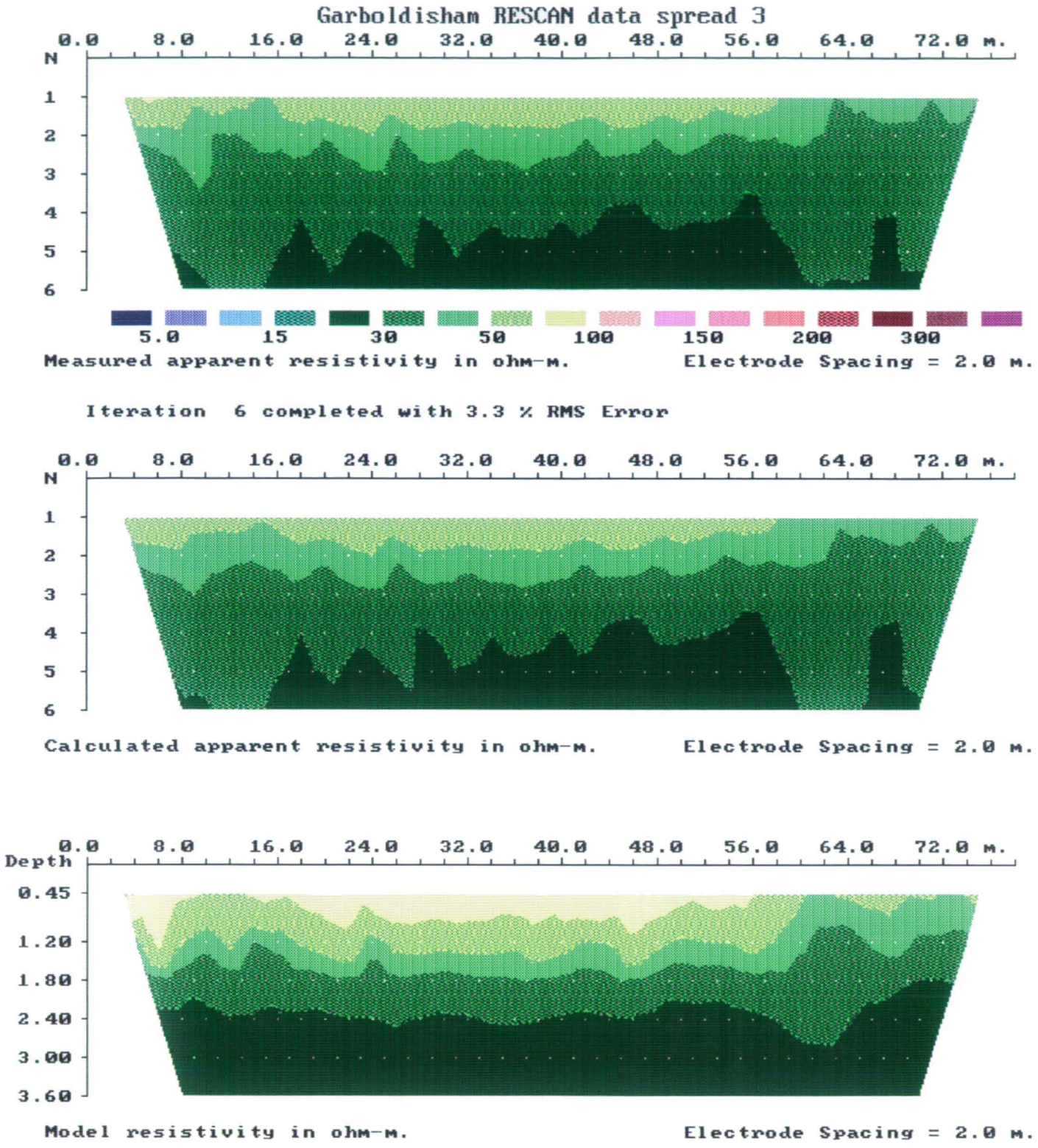

Figure 16. Interpretation results for RESCAN detailed dipole-dipole apparent resistivity measurements, spread 3 (142 - 220 m along line 1).

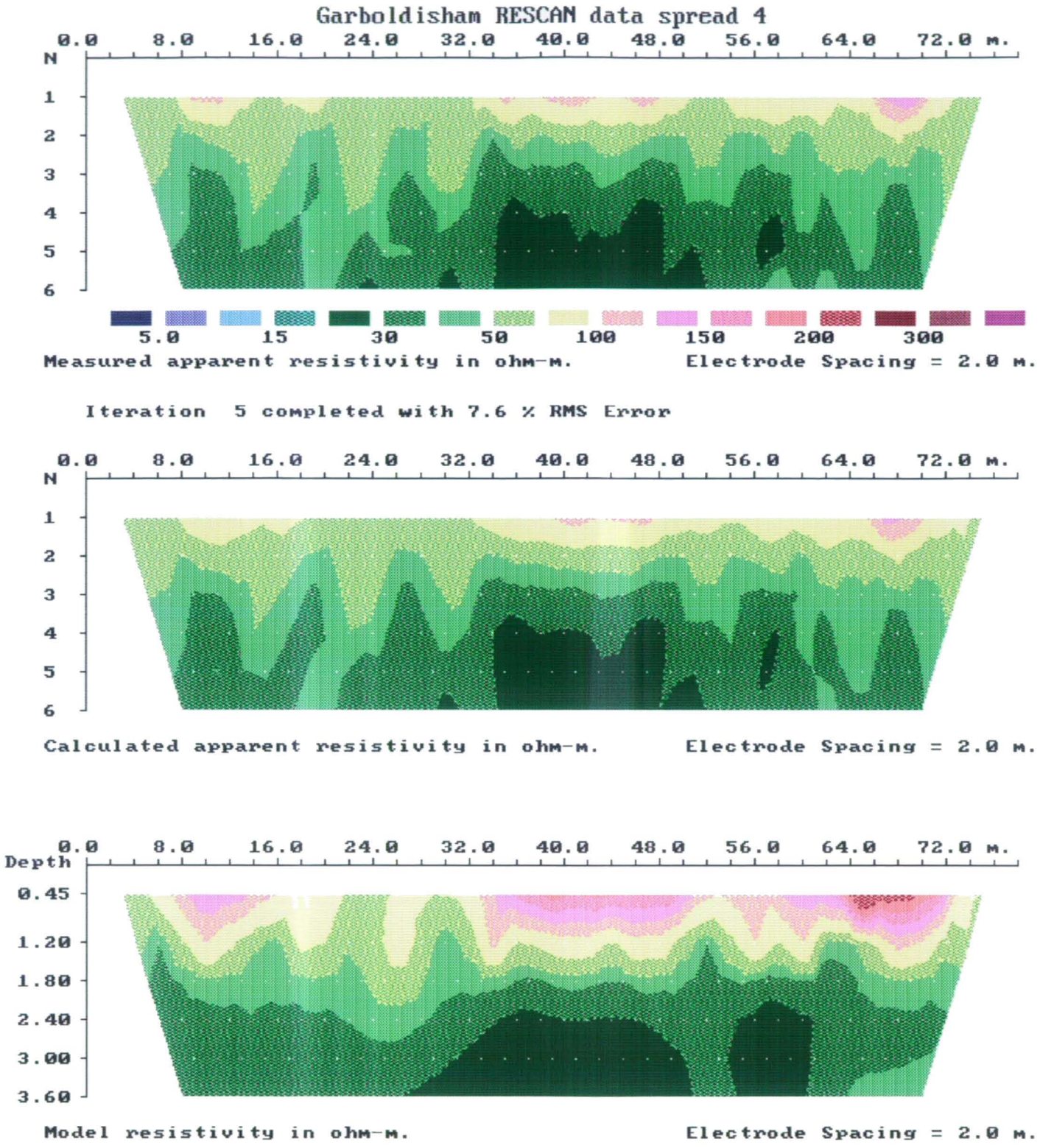

Figure 17. Interpretation results for RESCAN detailed dipole-dipole apparent resistivity measurements, spread 4 (60 - 138 m along line 2).

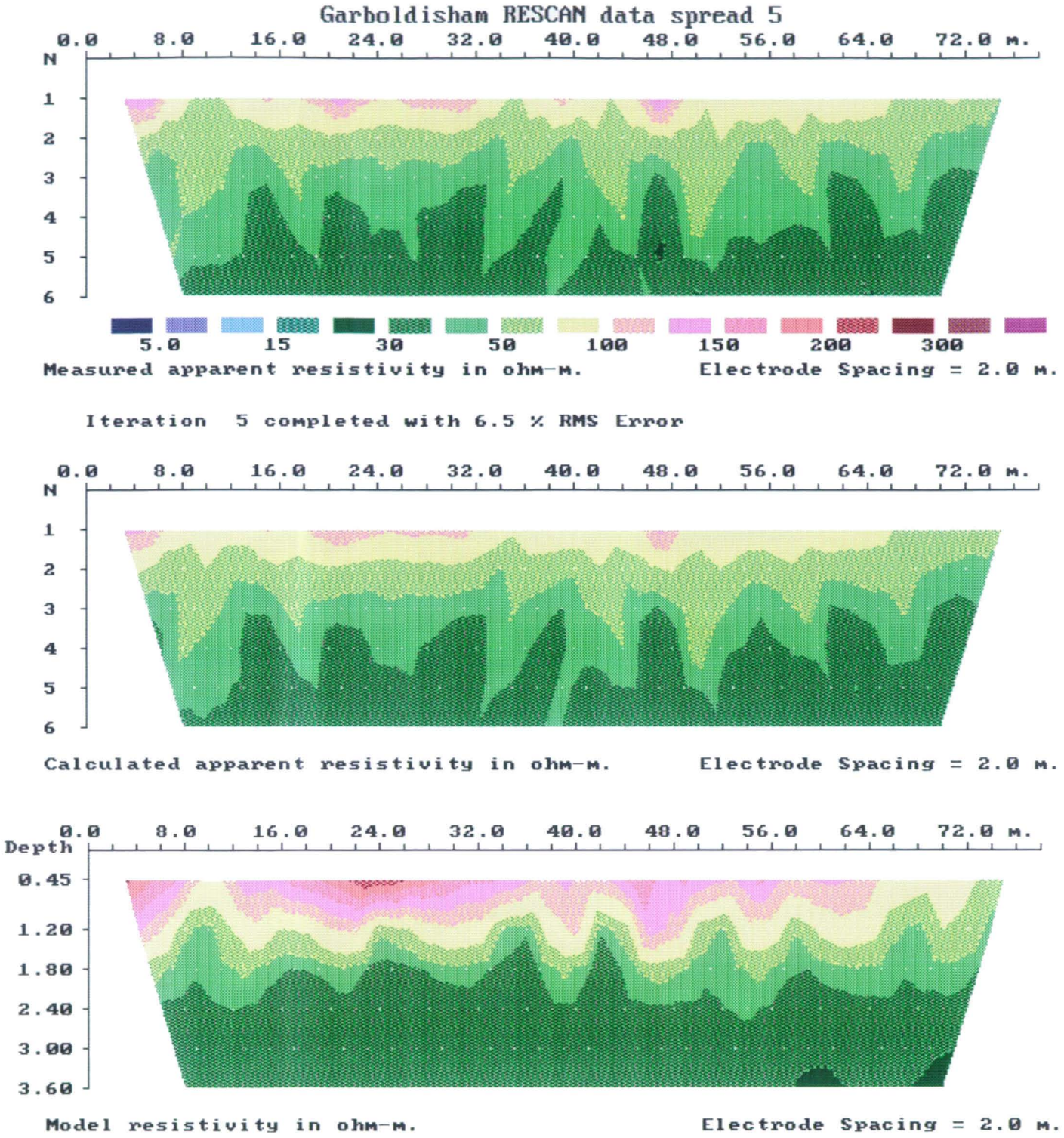

Figure 18. Interpretation results for RESCAN detailed dipole-dipole apparent resistivity measurements, spread 5 (124 - 202 m along line 2).

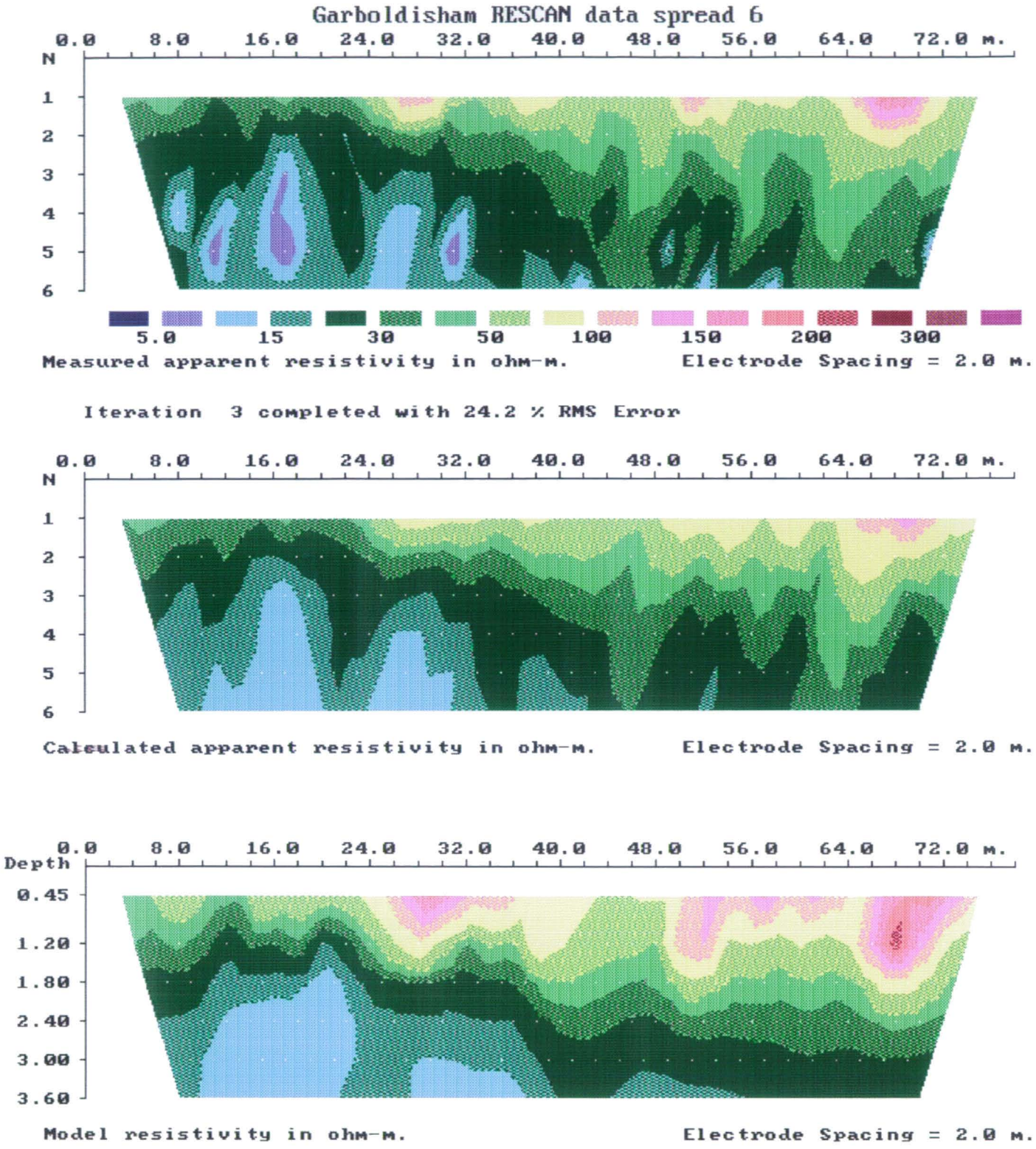

Figure 19. Interpretation results for RESCAN detailed dipole-dipole apparent resistivity measurements, spread 6 (60 - 138 m along line 3).

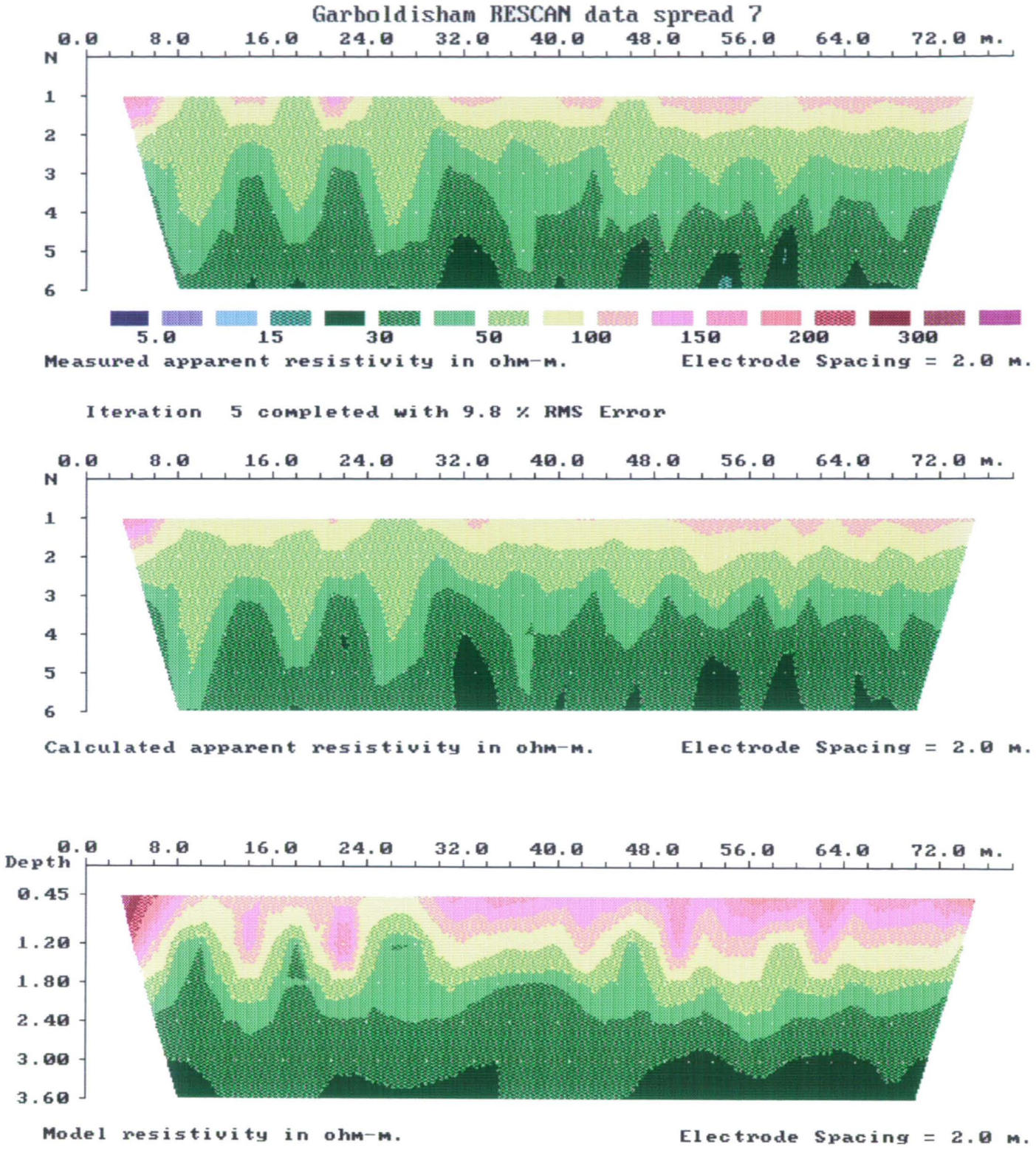

Figure 20. Interpretation results for RESCAN detailed dipole-dipole apparent resistivity measurements, spread 7 (124 - 202 m along line 3).

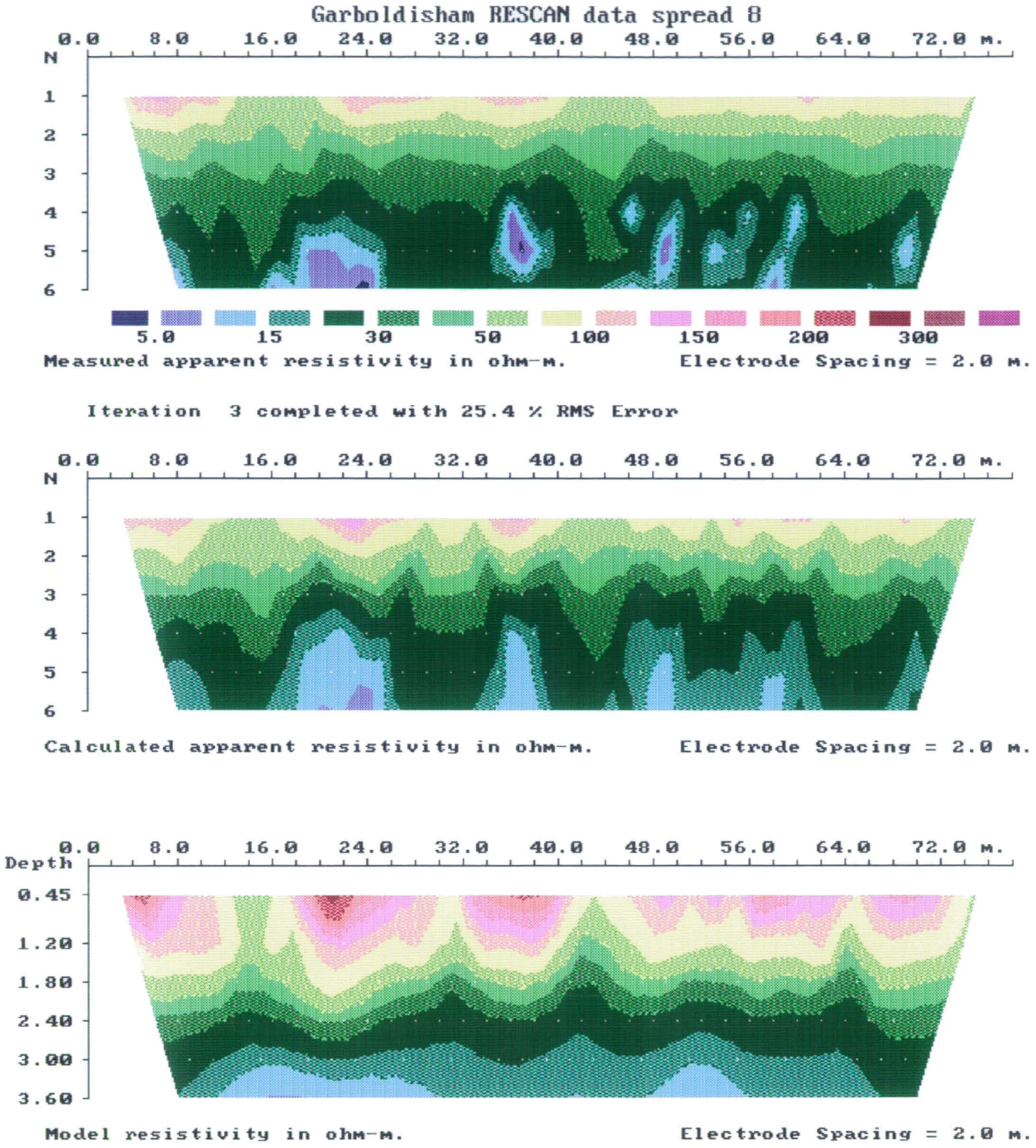

Figure 21. Interpretation results for RESCAN detailed dipole-dipole apparent resistivity measurements, spread 8 (124 - 202 m along line 4).

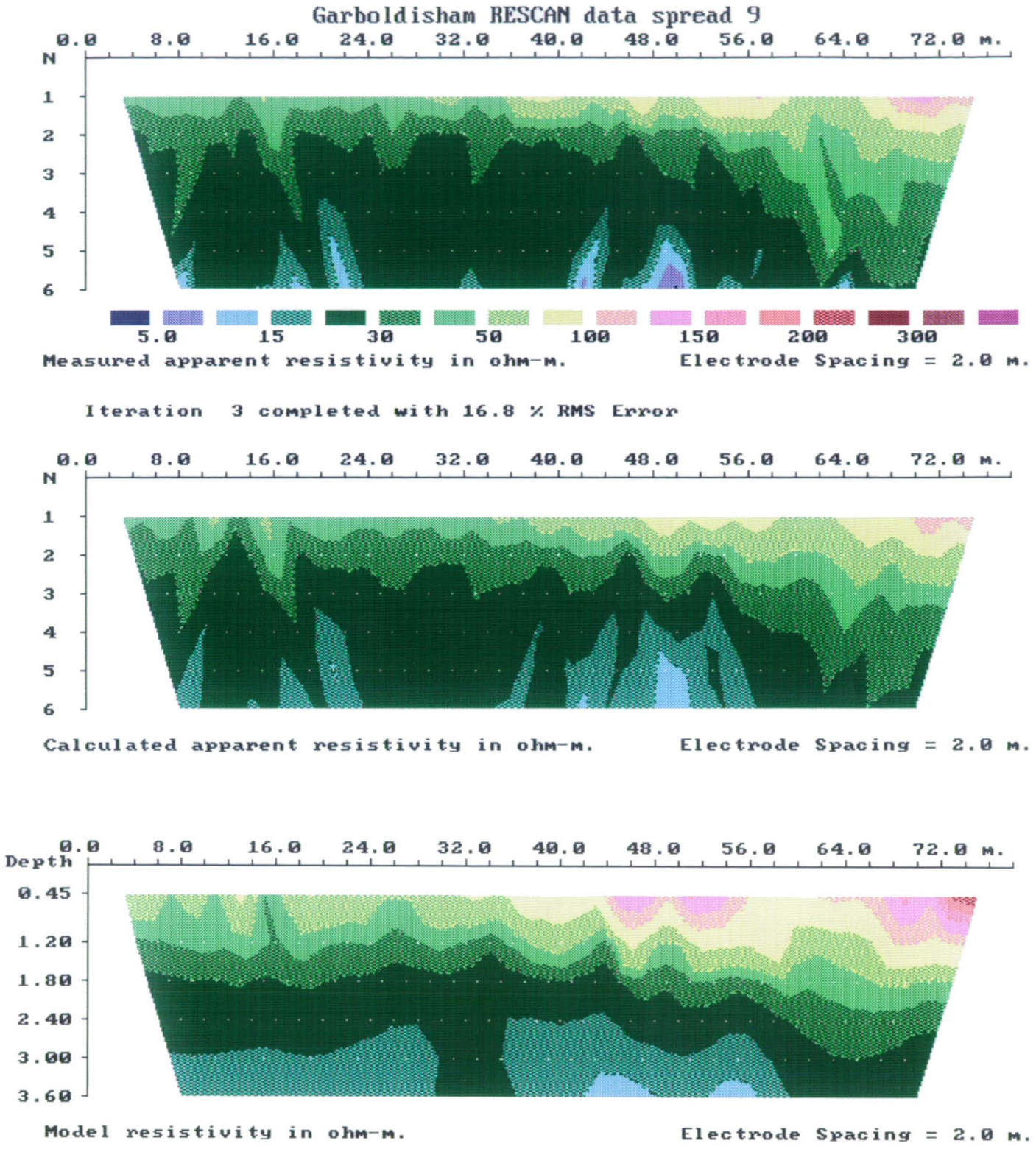

Figure 22. Interpretation results for RESCAN detailed dipole-dipole apparent resistivity measurements, spread 9 (60 - 138 m along line 4).

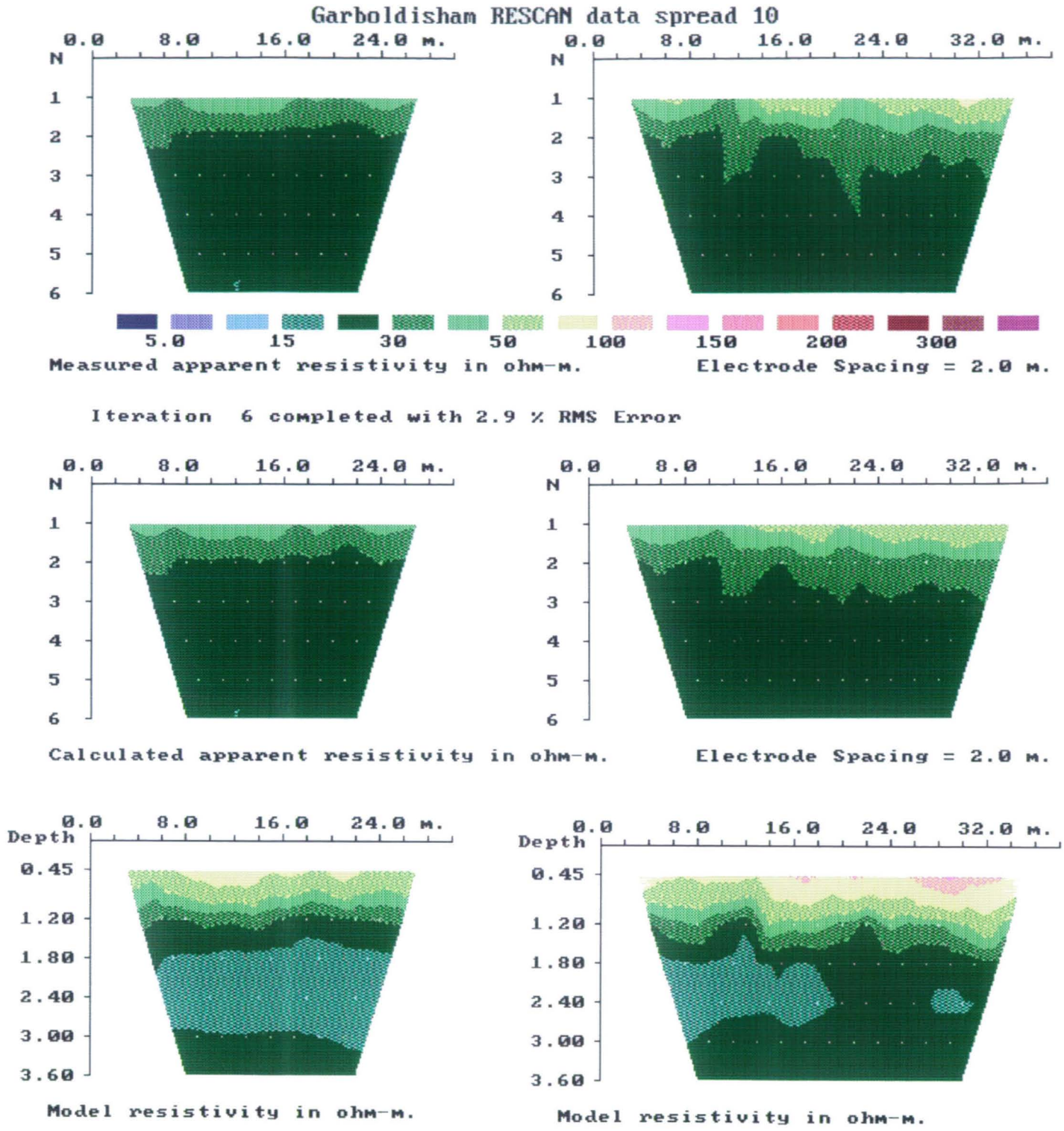

Figure 23. Interpretation results for RESCAN detailed dipole-dipole apparent resistivity measurements, spread 10, along line 5. Left hand section is from 60 - 90 m, right hand section is from 100 - 138 m.

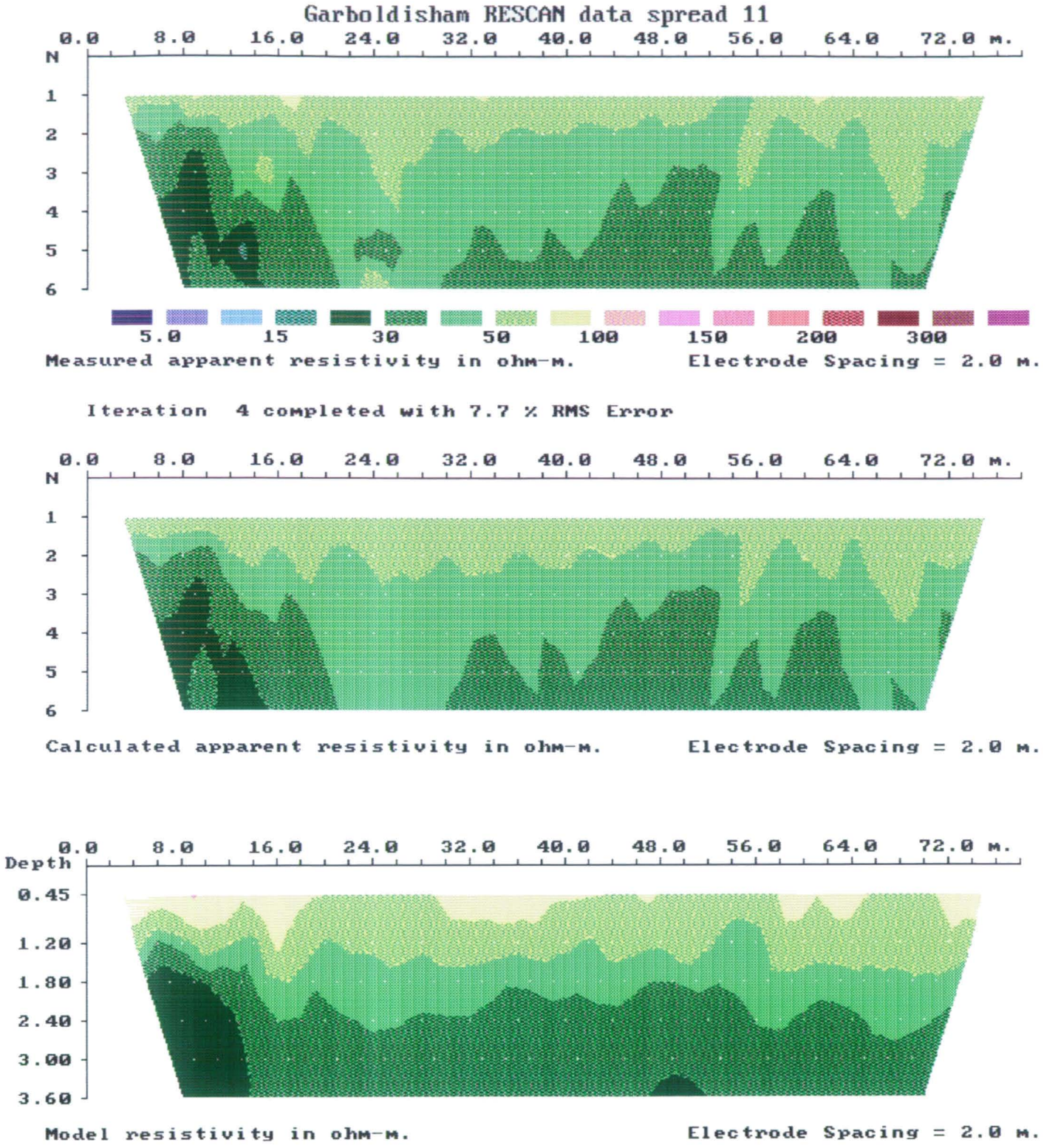

Figure 24. Interpretation results for RESCAN detailed dipole-dipole apparent resistivity measurements, spread 11 (124 - 202 m along line 5).

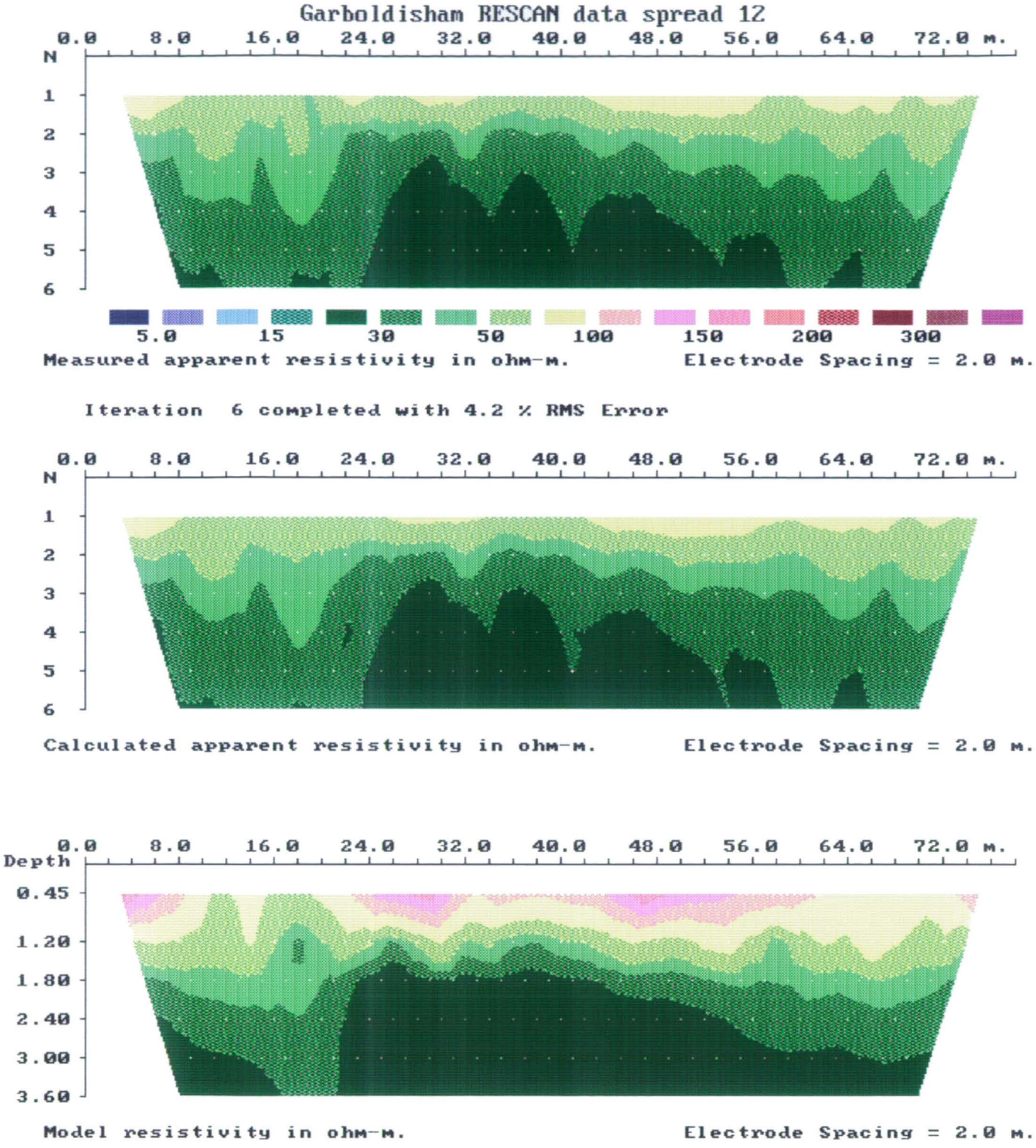

Figure 25. Interpretation results for RESCAN detailed dipole-dipole apparent resistivity measurements, spread 12 (124 - 202 m along line 6).

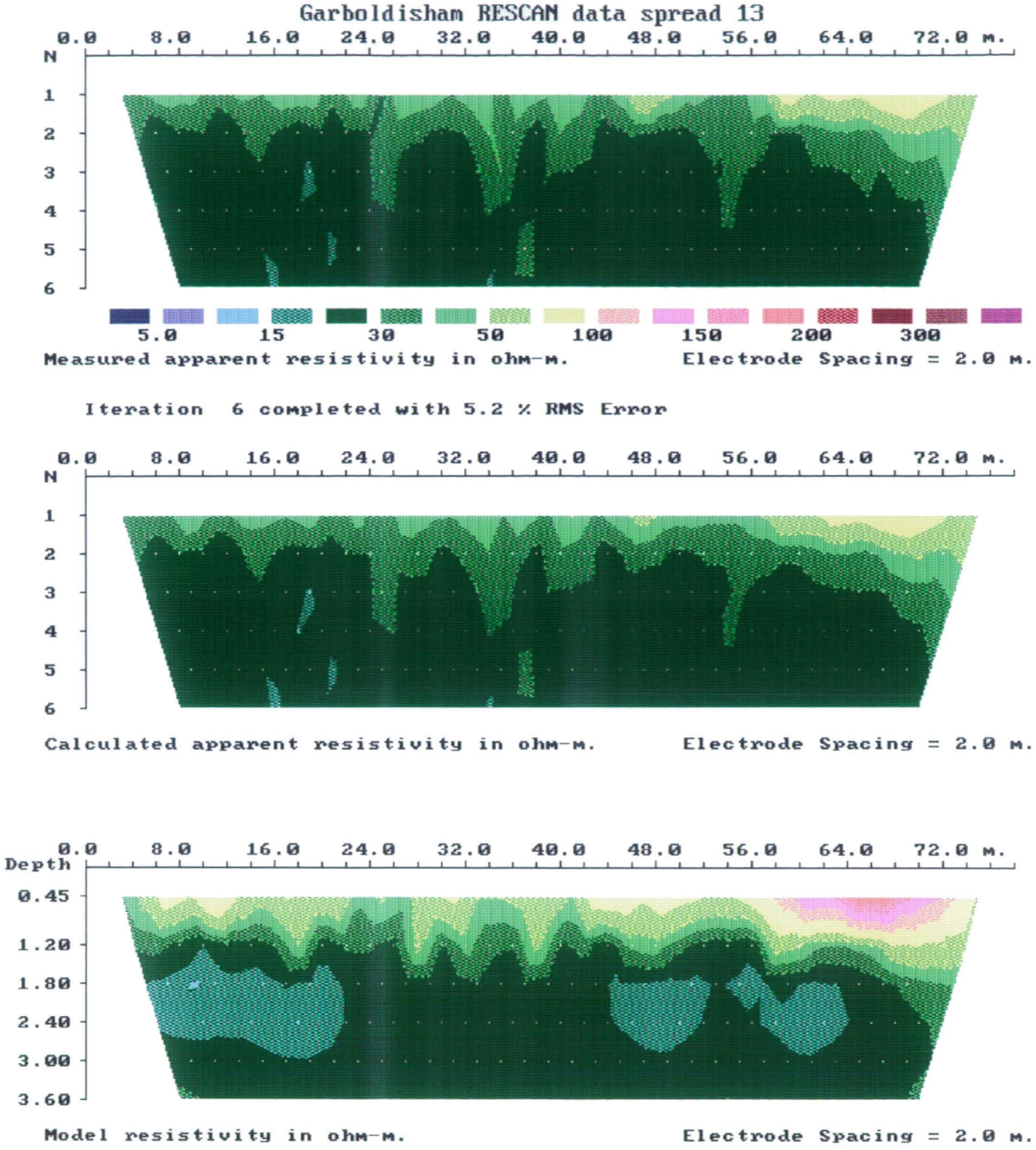

Figure 26. Interpretation results for RESCAN detailed dipole-dipole apparent resistivity measurements, spread 13 (60 - 138 m along line 6).

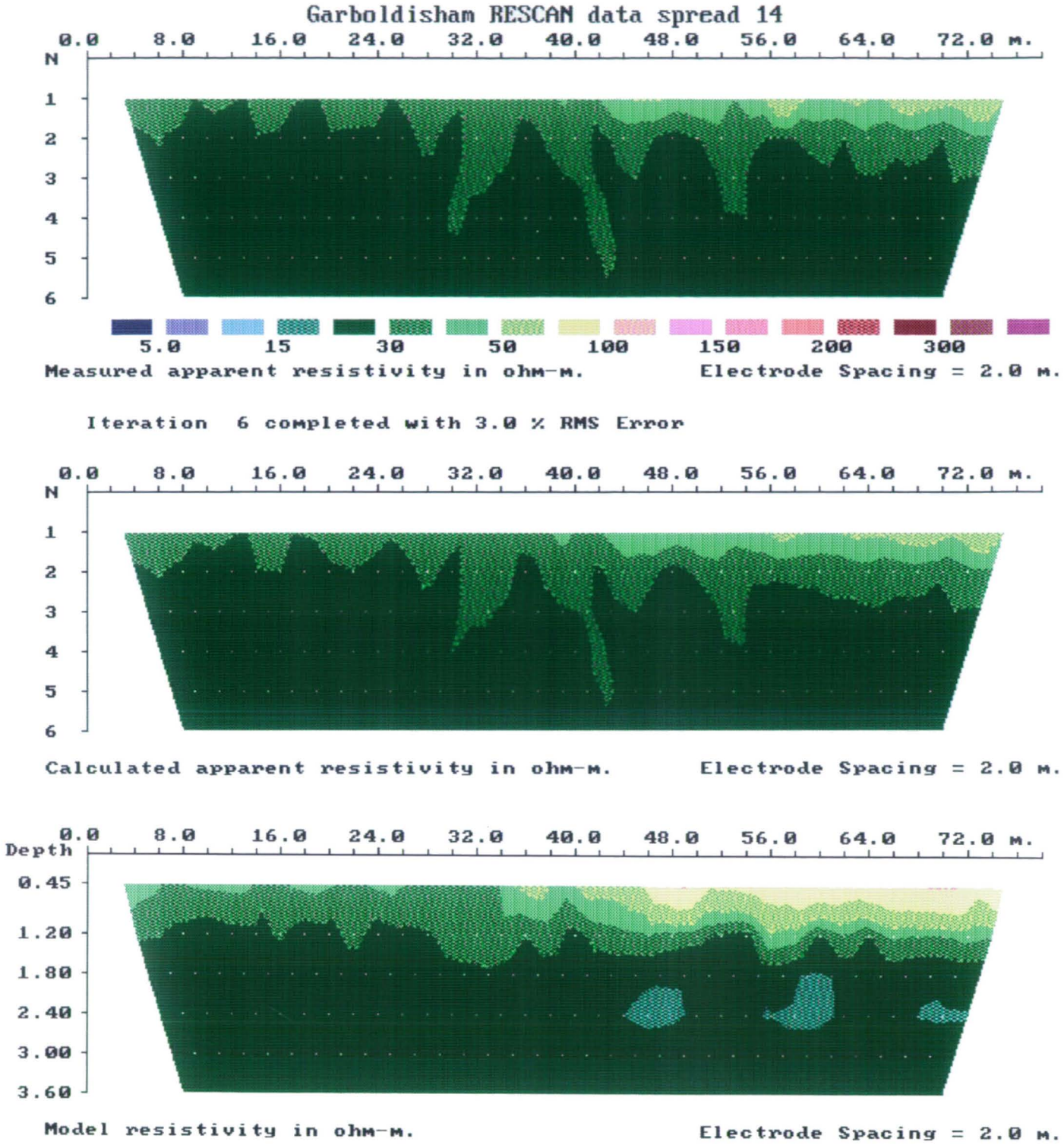

Figure 27. Interpretation results for RESCAN detailed dipole-dipole apparent resistivity measurements, spread 14 (60 - 138 m along line 7).

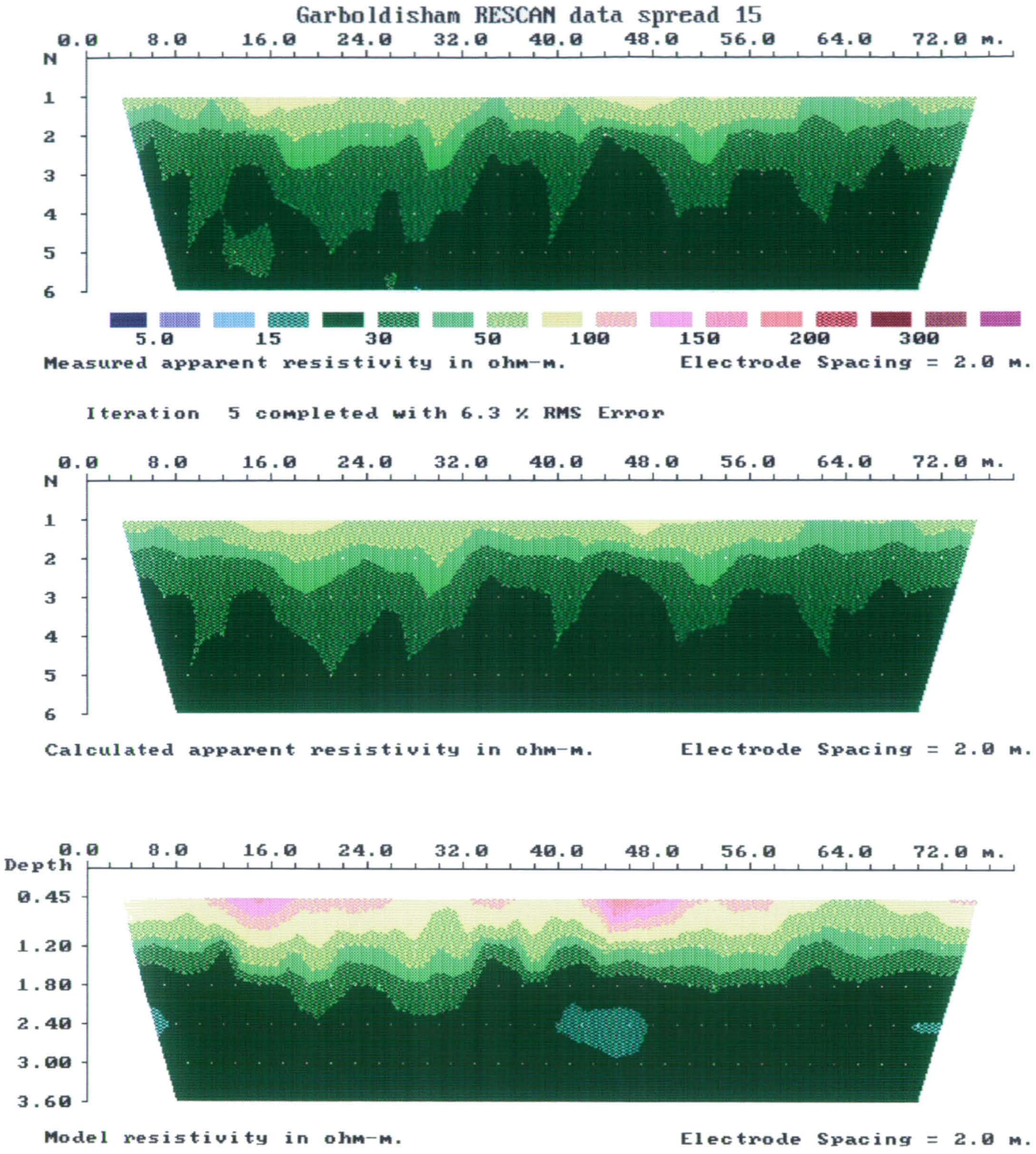

Figure 28. Interpretation results for RESCAN detailed dipole-dipole apparent resistivity measurements, spread 15 (124 - 202 m along line 7).

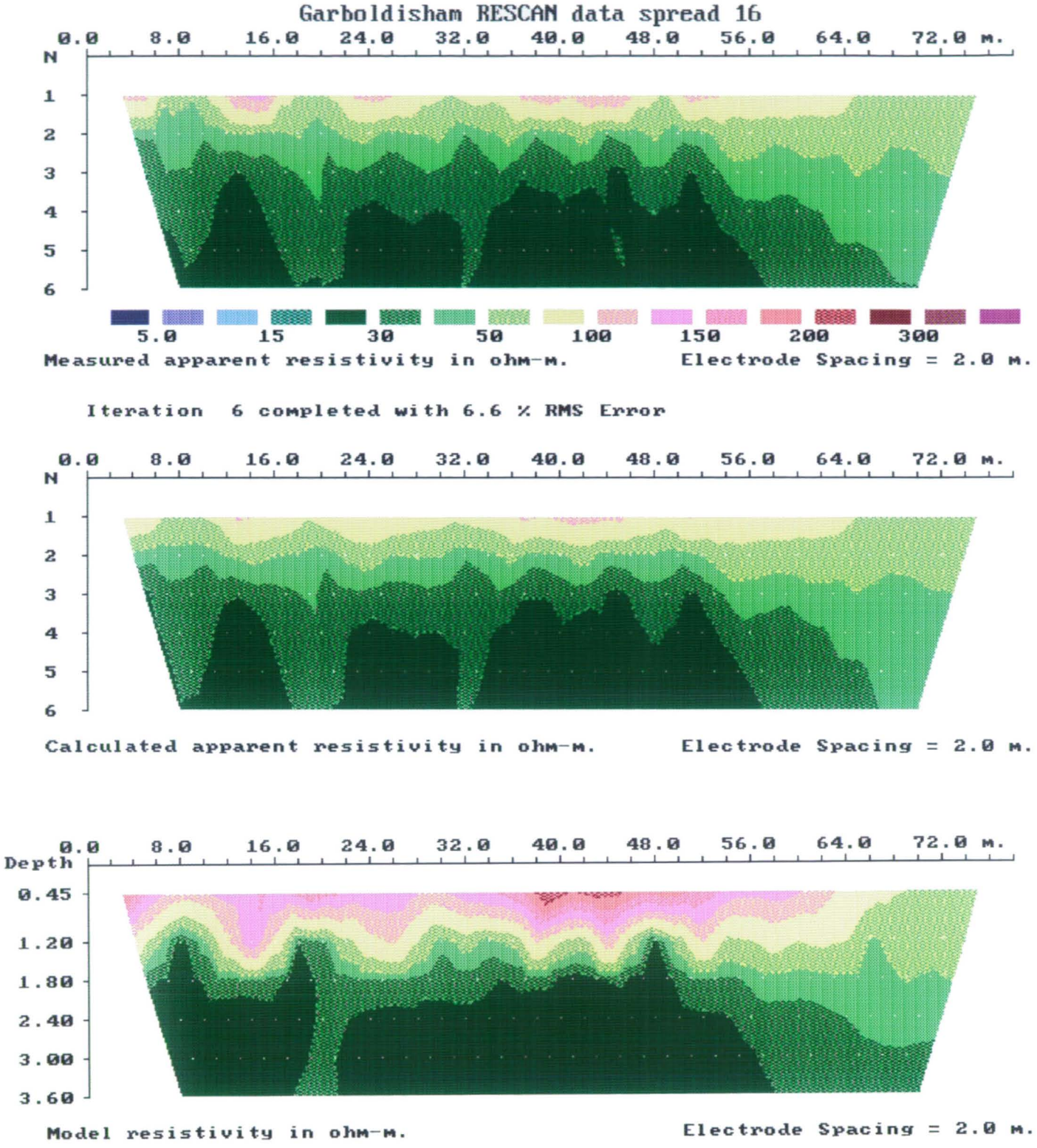

Figure 29. Interpretation results for RESCAN detailed dipole-dipole apparent resistivity measurements, spread 16 (124 - 202 m along line 8).

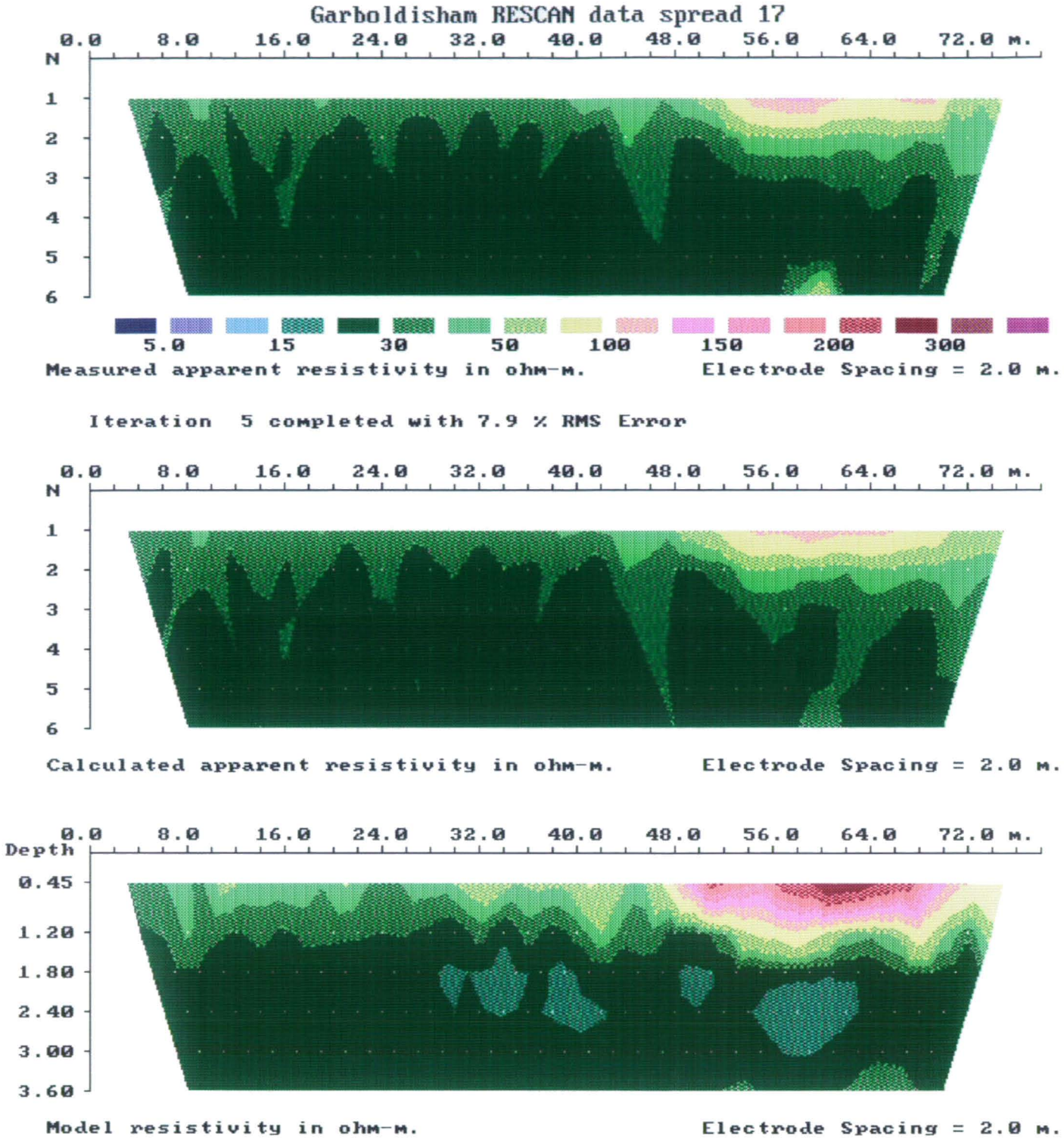

Figure 30. Interpretation results for RESCAN detailed dipole-dipole apparent resistivity measurements, spread 17 (60 - 138 m along line 8).

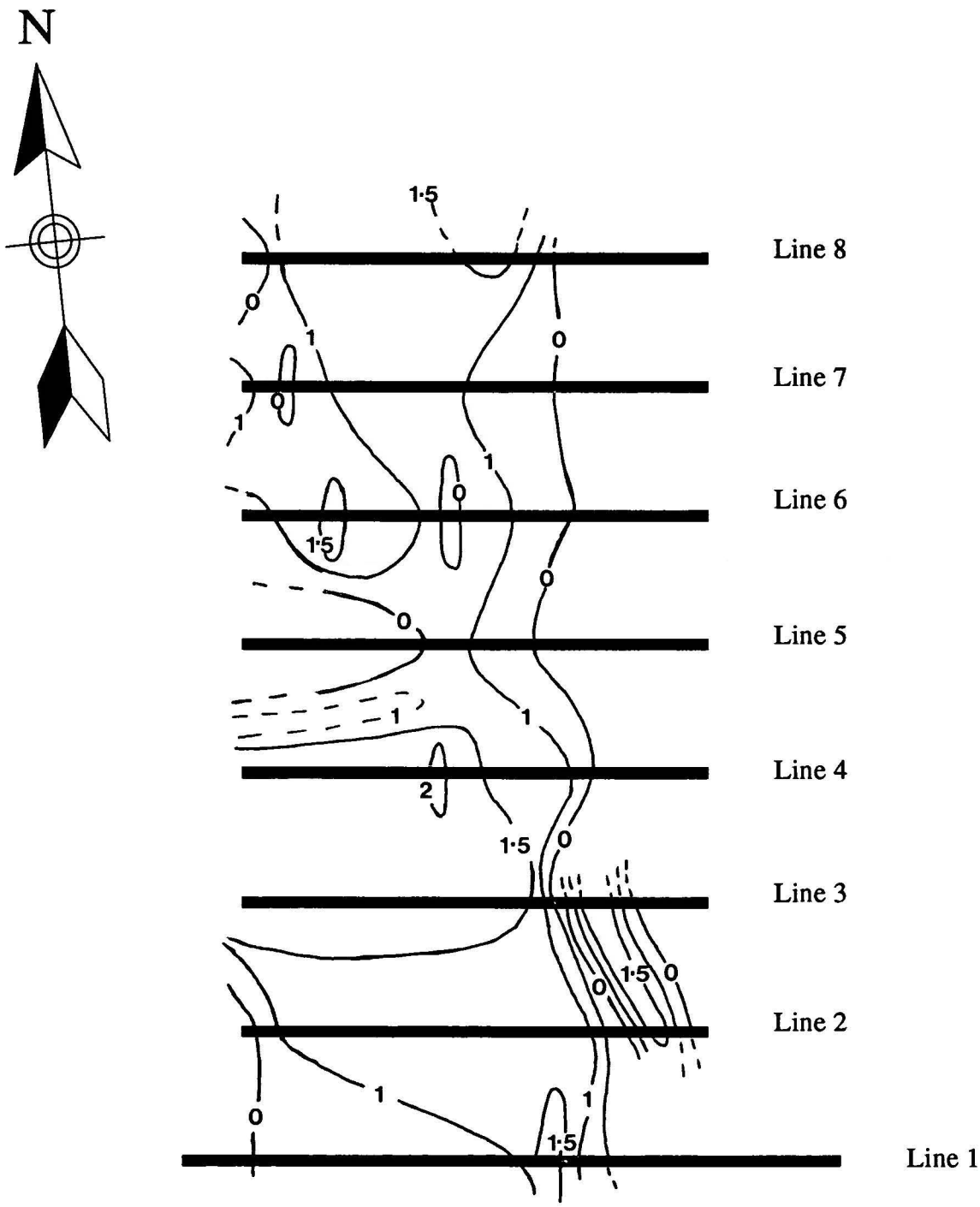

Figure 31. Contour plot of the depth to the base of the surface sand layer over the detailed apparent resistivity grid. Depths are in metres.